PN-ACE-941

THE GEOPHYSICAL INSTITUTE OF ISRAEL המכון הגיאופיסי לישראל
P O B 2286 HOLON 58122, ISRAEL, TEL 972 3 5576050, FAX 972 3 5502925 ,רח' המשביר 1 חולון

101378

# SEISMIC HAZARD AND VULNERABILITY IN THE ASHGABAT REGION

*FINAL REPORT*

**Covering the period March 13, 1995 - October 31, 1998**

**Submitted to**

**Human Capacity Development Bureau for Global Programs,**

**Field Support and Research U S Agency for International Development**

Principal Investigator Dr Avi Shapira
Grantee Institution The Geophysical Institute of Israel (GII)
Co-Principal Investigator Prof , Dr Batyr Karryev
Institution Scientific-Information Bureau, Institute of Seismology, Academy of Sciences of Turkmenistan (SIBIS AST)

Collaborators
Dr E Kanel, Dr Y Zaslavsky, Dr Y Gitterman, A Malitzky and U Peled, The Geophysical Institute of Israel
Dr E Esenov and A Pegov SIBIS AST, The Academy of Science of Turkmenistan

Project Number CA14-031
Grant Number TA-MOU-94-CA14-031

*US-AID GRANT PROJECT OFFICER MR. R. MOULINEX*

**Scientific Attache, U S Embassy, Tel-Aviv, Israel**

*DECEMBER 1998*

A

# TABLE OF CONTENTS.


| | | Page No |
|---|---|---|
| 1 | EXECUTIVE SUMMARY | 1 |
| 2 | RESEARCH OBJECTIVES | 2 |
| 3 | METHODS AND RESULTS | 3 |
| | 3 1 Quantification of Seismicity in the Ashgabat Region | 3 |
| | 3 2 Data Acquisition at the Geyokcha Station | 4 |
| | 3 3 Seismic Microzonation of Ashgabat | 5 |
| | 3 4 Seismic Hazard Assessments for Ashgabat by Application of the SvE Method | 6 |
| | 3 4 1 The SvE Method | 6 |
| | 3 4 2 Application of the SvE to Ashgabat | 7 |
| | 3 5 Vulnerability of Buildings to Ground Motions | 8 |
| 4 | IMPACT, RELEVANCE AND TECHNOLOGY TRANSFER | 9 |
| 5 | PROJECT ACTIVITIES | 10 |
| | 5 1 Meetings | 10 |
| | 5 2 Training | 11 |
| | 5 3 Publications | 11 |
| 6 | PROJECT PRODUCTIVITY | 12 |
| 7 | FUTURE WORK | 12 |
| 8 | ACKNOWLEDGMENTS | 12 |
| 9 | LITERATURE CITED | 12 |

Appendix A Seismotectonics and seismicity in the Ashgabat region

Appendix B Data acquisition at the Geyokcha station and estimation of source parameters

Appendix C Seismic microzonation in Ashgabat

Appendix D Dynamic parameters of typical buildings

## FIGURE CAPTIONS

Figure 1 Map of earthquakes with M>3 5 (including historical) and four seismogenic zones determined in the Ashgabat region

Figure 2 Distribution of fundamental frequencies estimated from H/V ratio of microtremors in Ashgabat

Figure 3 Uniform hazard acceleration spectra for the 4 seismic zones of Ashgabat

# 1 EXECUTIVE SUMMARY

Most of Turkmenistan is located within an area of strong earthquakes The most recent destructive earthquake (M=7 3) in 1948 completely destroyed Ashgabat and caused numerous deaths The goal of this research project is to evaluate the seismic hazard and assess the dynamic parameters of existing buildings These evaluations are to be implemented by the local authorities in risk assessments and in urban planning in order to mitigate the effects of the earthquakes that will eventually occur

The available geological, seismological and geotechnical information was compiled at SIBIS AST and jointly analyzed The seismological data include the most complete catalog of earthquakes in the Iran-Turanian segment, from 2000BC until 1997 (more than 70,000 events) and a thorough study of the macroseismic evidence of the 1948 earthquake The macro-seismic information of that and other earthquakes as well as the compiled earthquake catalogue were used to define the empirical correlation between energy classes, magnitudes, epicentral distances and seismic intensities These data were also used to identify four seismogenic zones that pose a serious earthquake hazard to Ashgabat New procedures for the analysis of temporal and spatial distributions of earthquakes within these zones were developed The newly installed seismic station at Geyokcha provided useful information that enabled us to develop correlation functions between the source parameters of local earthquakes, energy class and moment magnitudes In turn, these were used to estimate frequency-magnitude relationships for the four seismogenic zones

Within the framework of this project we developed software for PC-based data acquisition (PC-SDA) and data processing (GII-SDP and GII-SRD) Microtremor measurements were conducted at various locations across Ashgabat from which we have estimated the site response functions These functions are associated with geological and geotechnical information to provide the seismic microzonation map of Ashgabat The above mentioned evaluations are integrated through the new SvE method to yield uniform hazard site specific acceleration spectra for the four seismogenic zones These acceleration spectra (often referred to as design acceleration spectra) are the main seismological data to be used in earthquake resistance building design

In order to enhance the earthquake risk assessment capability for the existing buildings in Ashgabat, we instrumented a number of typical tall buildings and defined their basic dynamic parameters, namely the fundamental resonance frequency and corresponding damping ratio Evidently, the proximity of the building's resonance frequency to the peak spectral accelerations of ground shaking is the main cause of heavy destruction and casualties

The project studies were carried out through close cooperation between the Academy of Science (SIBIS AST) of Turkmenistan and the Seismology Division of the Geophysical Institute of Israel (GII), based on joint meetings and workshops held both in Israel and Turkmenistan as well as joint field operations in Ashgabat An important part of the activities involved lectures and seminars for the administration and the engineering community of Ashgabat

The Israel team developed and transferred to SIBIS AST software packages to support data acquisition, calibration procedures, assessment of earthquake source parameters and complicated algorithms for engineering estimations Turkmenian researchers were trained at the GII to use and maintain the hi-tech equipment and to apply innovative methods of seismic monitoring and site-response evaluation Three modern PC-based data acquisition systems were purchased and assembled at GII facilities and shipped to Turkmenistan The new seismic equipment and software provided crucial upgrading of the existing monitoring capabilities in Turkmenistan and was used for empirical evaluation of site response and dynamic characteristics of buildings in various parts of Ashgabat

## 2. RESEARCH OBJECTIVES

The overall aim of the project is to contribute to the mitigation of the earthquake hazard to Ashgabat, the capital of Turkmenistan, and to upgrade the seismological capability of the Central Asian republic of Turkmenistan In the course of this project we emphasized the following research objectives

1 Identification of the main seismogenic zones and evaluation of the spatial and temporal distribution of earthquakes in and around Ashgabat Up-to-date fractal analysis procedures were applied to derive the mathematical expressions of these distributions The fractal dimensions of the local and regional seismicity contribute to a better understanding of and quantify the tectonics and nature of earthquakes in the Central Turkmenistan region

2 Seismic microzoning of Ashgabat based on compiled geological and geotechnical data of Ashgabat and empirical evaluations of the site response using Nakamura and "receiver function" techniques

3 Assessment of the seismic hazard in different parts of the city The seismic hazard is quantified here in terms of the uniform hazard site specific acceleration spectrum computed for a probability of occurrence of 10% in an exposure time of 50 years and for a damping ratio of 5% Computations were made using the newly developed SvE procedure

4 Empirical determinations of the dynamic properties of structures in Ashgabat by analyzing its response to ambient vibrations

5 Upgrading the existing seismic monitoring capabilities in the region The project has enhanced the technological capabilities of Turkmenistan by providing seismic instruments, training and newly developed software for seismological monitoring and analysis

# 3 METHODS AND RESULTS

## *3 1 QUANTIFICATION OF SEISMICITY IN THE ASHGABAT REGION*

The initial stage in every seismic hazard analysis is the compilation of the geological and seismological information that is relevant to the investigated region The results of our efforts in this field are summarized in Appendix A The seismic activity in the central part of the Kopetdag is associated with the dynamics of the interaction between Turanian and Iranian plates The seismotectonics of this region are complicated, however, a detailed analysis of geological data complemented by detailed studies of the seismic history of the area and its macroseismic effects (especially during the destructive earthquake in 1948), were used to construct tectonic models for the region An important source of information was the seismological bulletin completed with new data acquired in the course of the project While previous studies deal mainly with a qualitative description of the seismicity in the region, the instrumentally obtained seismic data were helpful in describing the seismicity in quantitative terms

In the current study we have attempted to quantify the spatial and temporal distribution of earthquakes in and around Ashgabat in fractal dimensions Appendix A also presents the fundamentals of the fractal analysis implemented in this study The analysis lead to the identification of four seismogenic zones that pose the main seismic hazard to the city of Ashgabat the Ashgabat, Germab, Bodgnurd and Quchan areas (see also map in Fig 1) The geographical boundaries of these seismogenic zones, the focal depth distribution in each zone and the fractal dimension D that is associated with the spatial distribution of the activity in each of them, are given in Table 1

**Table 1 Seismogenic Zones Defined in the Ashgabat Region**

| Seismogenic zones | Latitude, deg. | Longitude, deg | $a_1$ | $b_1$ | A | B | Depth km | $D_s$ |
|---|---|---|---|---|---|---|---|---|
| Ashgabat | 37 35-38 3 | 58 0-58 70 | 2 32 | -0 459 | 2 521 | -0 484 | 10-20 | 1 52 |
| Germab | 37 7-38 60 | 57 3-57 75 | 2 791 | -0 46 | 3 011 | -0 483 | 5-10 | 1 38 |
| Bodgnurd | 37 0-37 65 | 57 0-58 15 | 3 113 | -0 466 | 3 372 | -0 488 | <50 | 1 59 |
| Quchan | 37 0-37 65 | 58 3-59 00 | 2 306 | -0 369 | 2 577 | -0 406 | <50 | 1 63 |

It is interesting to note that while analyzing the temporal distribution of earthquake activity in the Ashgabat region, it was observed that a major shock is usually preceded by a maximum D value and followed by a minimum Major shocks were defined as earthquakes whose energy class exceeds the threshold energy class (see Table A3 in Appendix A) for 4-5 units For time intervals without "main" shock, the fractal dimension showed "quasi constant" behavior, nevertheless the long term seismic activity can be characterized in the time domain by adhering to the classic Guttenberg-Richter frequency-magnitude relationship Since earthquake strength is traditionally quantified in Turkmenistan in terms of Energy classes K, we computed the frequency-K relationships for incremental (n) and cumulative (N) functions i e

$$\log n = b_1*(K-8)+a_1 \quad (1)$$

$$\log N = B*(K-8)+A \quad (2)$$

The best fit of parameters $a_1$, $b_1$, A and B, for each of the seismogenic zones are also presented in Table 1

### *3 2 DATA ACQUISITION AT THE GEYOKCHA STATION*

Through the joint efforts of both teams, a permanent seismic station was installed in Geyokcha, near Ashgabat The data acquired by this station are used in the evaluation of dynamic parameters of local and regional earthquakes The station was tested, tuned and calibrated by Israel specialists during July 1996 A year later, a set of new L4C 3C seismometers (Mark Products) was installed at the station, replacing the old Russian seismometers Data acquisition was facilitated using the PC-SDA system (see Shapira and Avirav, 1995) Data processing of the recorded events was carried using on a new PC-based software package GII-SDP (Seismic Data Processing package, designed and written by

Malitzky and Shapira, 1996) Both software packages were developed and modified within the framework of this project

Despite severe logistic difficulties, the station recorded 18 earthquakes with magnitudes up to $m_b$=3 8 which occurred in close proximity to Ashgabat The list of events, their source parameters and the velocity model used for their location are tabulated in Appendix B The magnitude $m_b$ was estimated from the relation (Karryev, 1992)

$$m_b = (K - 2\ 7)/1\ 7 - 0\ 17 \qquad (3)$$

The seismic moment estimations, $M_0$ follow the Brune omega square model (Brune, 1970) As demonstrated by Nafi and Shapira (1998) and Feldman et al (1998), we may adhere to the equation of Hanks and Kanamori (1979) to define a local magnitude, $M_m$

$$M_m = -10\ 6 + 0\ 6667 \log(M_0) \qquad (4)$$

where $M_m$ is the moment magnitude estimated from seismic moment determinations that are based on short period recordings only

Following this procedure, we obtained a good correlation between the energy class determinations K (traditionally used in Turkmenistan) and the new magnitude scale (see also Appendix B)

$$M_m = 0\ 372\ K + 0\ 152 \qquad (5)$$

Apart from the general significance of being able to determine local magnitudes (rather then K) in Turkmenistan, we had to verify that the theoretical attenuation with distance, $R^1$, of the zero-frequency spectral amplitudes of the S wavetrain, is applicable in the study area Hence, based on the earthquake records of the Geyokcha station, we can apply equation (5) and the attenuation function $R^1$, in the application of the SvE method for estimating the seismic hazard in Ashgabat

### *3 3 SEISMIC MICROZONATION OF ASHGABAT*

Nowadays it is evident that local site conditions dominate the distribution of damage within the area affected by an earthquake A major part of our project, at least in terms of field operations, was to define site response functions for different locations across Ashgabat and associate them with the geological and geotechnical local information and macroseismic

evidence, to yield a seismic zonation map of Ashgabat Details of the studies associated with this task, including seismic measurements and site response determination at 56 locations in Ashgabat, are presented in Appendix C

As shown on the map in Fig 2, we have divided Ashgabat into four zones, each of them characterized by a typical subsurface model (see Table C5 in Appendix C) These models are to be integrated in the SvE computations for determining synthetic site-specific accelerograms

## *3 4 SEISMIC HAZARD ASSESSMENTS FOR ASHGABAT BY APPLICATION OF THE SvE METHOD*

### 3 4 1 The SvE Method

Modern practice in designing buildings to withstand earthquakes is to apply a modal analysis while taking into account the expected accelerations and displacements that will be caused to the building due to ground shaking This practice is also applied in many modern building codes To comply with this engineering practice, seismologists are required to provide the acceleration response spectrum, i e , the spectrum of accelerations (or displacements) of a series of single degree of freedom (natural frequency) oscillators (buildings) and a specific damping

The SvE method (Shapira and van Eck, 1993) was developed to comply with those requirements It is designed to provide the uniform-hazard, site-specific acceleration response for a prescribed probability of occurrence (exceedance of spectral accelerations) and a given damping ratio of the building The SvE computations are based on regional parameters such as distribution of seismogenic zones, frequency-magnitude relationships, stress drop, Q-values, seismic moment - magnitude relationship, etc The uncertainties associated with these parameters are incorporated in the SvE by applying Monte-Carlo statistics, i e , simulating several possible lists of earthquakes over a very long time and synthesizing many accelerograms The regional information is used to synthesize accelerograms for the surface of the bedrock underlying the site Computations are based on the Stochastic method (Boore, 1983, Boore and Atkinson, 1987) and are then convoluted with the response function of the site under investigation to yield the expected accelerations on the free surface of that site using the Joyner computer code (1977) The huge data set of synthetic accelerograms is used to compute the acceleration response for a given

damping ratio and then the spectral accelerations that corresponds to a prescribed probability of exceedance The latter are computed under the assumption that, in a given site, the temporal distribution of the logarithm of acceleration level at a given frequency follows Poisson distribution laws

3 4 2 Application of the SvE to Ashgabat

As stated above, our studies of the seismicity of the area result in the definition of four seismogenic zones We used the seismicity parameters associated with each zone to generate artificial catalogues of earthquakes that may occur over a period of 5000 years The seismicity over such a long period is not necessarily stationary and, therefore, each catalogue reflects the probabilities of earthquake occurrences over a much shorter period (e g 50-100 years) and does not necessarily describe the seismicity over 5000 years In the process of preparing the various earthquake catalogues, we assumed that the location of the hypocenters was uniformly distributed within the geographical boundaries of the seismogenic zones and the defined range of focal depths Different catalogues are simulated for different seismicity parameters, i e , we estimated, rather conservatively, that the number of events $n$ of a certain energy class that will occur over 5000 years is uncertain within three times the square root of $n$
In synthesizing accelerograms we adhered to the Brune (1970) model and applied the following assumptions

a) The conversion of K to seismic moment follows equations (4) and (5) The estimated seismic moment is log normally distributed with an uncertainty factor of 2 (one standard deviation)

b) The attenuation of the zero-frequency displacement level with distance R is $R^{-1}$ We added an inelastic attenuation in the form

$$Exp[\frac{-\pi f R}{QV}]$$

where $f$ is the frequency of vibration, V=3 6 km/sec and Q is uniformly distributed between 50-150

c) The stress drop is assumed to be uniformly distributed between 50 and 100 bar

d) $f_{max}$ is uniformly distributed between 8 and 15 Hz

It should be understood that our estimations regarding the values of Q, stress drop and $f_{max}$ are based on "best judgement" since we do not have sufficient data to derive these values from in-situ observations Consequently, we also had to choose a rather wide range of uncertainty intervals

The uniform hazard acceleration spectra for each of the seismic zones of Ashgabat, are presented in Fig 3 These functions are computed for an exceedance probability of 10% in an exposure time of 50 years and for a damping ratio of 5% These criteria are commonly used in most modern building codes

### *3 5 VULNERABILITY OF BUILDINGS TO GROUND MOTIONS*

A detailed engineering analysis of the vulnerability of a building to ground motions caused by an earthquake is beyond the scope of this project We have focused our interest on determining empirically the basic dynamic parameters of typical buildings as described in Appendix D The main results of that analysis are

a) As a first approximation, the resonance frequency of pre-fabricated multistory building in Ashgabat can be estimated by the relationship

$$f=23/N \qquad (6)$$

where N is the number of stories

b) The damping ratios for existing buildings in Ashgabat are of the order of 2 5%-3 5%, indicating relatively low stiffness For comparison, modern building codes consider a damping ratio of 5%

c) The resonance frequency of old masonry buildings in Ashgabat is of the order of 8 Hz with a corresponding damping ratio of ~3 5%

Frequencies at the maximum of the uniform hazard acceleration spectra (see Fig 3) correspond to the distribution of fundamental frequencies estimated from microtremor measurements Enhanced damage occurs if a structure has a natural frequency almost the same as the natural frequency of the site on which the building rests "Double resonance" of both the site and the building can occur in this case The empirical formulae (6) proposed for calculating the fundamental frequencies of multi-story buildings combined with the estimated dominant site frequencies (see Figs C8 and C9) are a basic ingredient for vulnerability assessment of existing buildings, and can contribute to the planning of seismic risk reduction for future construction in Ashgabat

## 4. IMPACT, RELEVANCE AND TECHNOLOGY TRANSFER

GII has developed software packages PC-SDA, PC-SIR, GII-SDP and GII-SRD that were transferred to Turkmenistan and installed on the computers in Ashgabat and jointly used by the Israeli and Turkmen teams The PC-SDA (PC-based Seismic Data Acquisition system) was used extensively for earthquake monitoring at the Geyokcha station, in site response investigations and in the measurements of the dynamic characteristics of buildings The PC-SIR software was also required for determining the seismic instrument response functions at every session of field measurements The GII-SDP (Seismic Data Processing) and GII-SRD (Site Response Determinations) were developed for processing the acquired seismograms

The multi-channel, PC-based, digital data acquisition monitoring system was specifically designed and developed for this project and applied in Turkmenistan The seismic acquisition system is operational and will probably be used to intensify site response measurements and determine dynamic parameters of buildings

This project also called for the establishment of communication links between the collaborating institutions Therefore, new equipment (PC-586 Acer and Fax-modem US Robotics) were installed and used widely by SIBIS AST for Internet site support, e-mail and data exchange with GII and other institutions around the world A SIBIS AST "home-page" was developed to serve the scientific collaboration between the Israeli and Turkmen seismologists It also provided free access to the seismic data used in our project

In order to facilitate field measurements in Turkmenistan we found it necessary to replace the existing seismometers with a new set of three short period seismometers produced by Mark Products, USA In addition to the seismometer, the SIBIS AST is equipped with a three-component, digital accelerometer (Kinemetrics, USA) This accelerometer was installed in the same deep vault in Geyokcha and connected to the PC-SDA Unfortunately, no earthquake caused strong enough ground motions to be triggered by this accelerometer The

seismic equipment, arranged as Mobile Recording Complex (MRC), installed in the host country, is a significant improvement on the existing monitoring capabilities in the Central Asian region

During the field work we were confronted with serious problems with the power supply to the computers and seismic equipment Hence, we acquired a generator (Robin R650) that was used throughout the project to perform measurements All the equipment purchased and installed during the project remains in Turkmenistan and will be used for future seismological and seismo-engineering studies in the region

## 5. PROJECT ACTIVITIES

### *5 1 MEETINGS*

5 1 1 The first meeting between the principal investigators took place in Ashgabat shortly after the project was approved by the US-AID It also included meetings with the administration of the Academy of Science of Turkmenistan and the municipality of Ashgabat at which the main objectives of this project were presented

A Workshop entitled "Evaluation of potential hazardous seismic zones in the Ashgabat region" was organized by the SIBIS AST, during July 1996 The main topics discussed during this workshop were

- Seismic activity and neotectonic in the Ashgabat region
- Methods and techniques for seismic data acquisition by MRC
- Processing of the seismological data
- Modeling of seismic activity by means of fractal analysis

5 1 2 As part of the Workshop, the SIBIS AST organized a scientific seminar for the Turkmen Academy of Sciences The seminar included a presentation of the project and its objectives, application of its expected results, a demonstration of the MRC, a demonstration of data processing and a review of new concepts in earthquake hazard and risk evaluation (including the SvE) Many Turkmenistan officials, scientists, experts and businessmen took part in the seminar

5 1 3 The project investigators participated in the NATO-ARW-951521 Workshop on "Historical and Pre-historical Earthquakes" (July 11-15, 1996 at Erevan, Armenia)

5 1 4 Based on the project results, two papers were presented in the XXVI General Assembly of the European Seismological Commission in Tel-Aviv, August 23-28, 1998

## *5 2 TRAINING*

Turkmen scientists (Prof B Karryev, Dr E Essenov and A Pegov) were trained to operate, calibrate and maintain the new equipment (MRC) The newly developed software was demonstrated and exercised Due to personnel changes in the Turkmen team it was necessary to repeat training and provide guidance to new people and to write an additional manual (in Russian) for the operation of the data acquisition system

Unfortunately, technical and economical problems in Turkmenistan have affected the ability of SIBIS AST to perform field measurements, maintain communication links and exchange data and information In July 1997 another Israeli team went to Ashgabat to exchange data, help in performing maintenance of the systems and assist in field measurements

## *5 3 PUBLICATIONS*

Shapira, A , Kanel, E and Karryev, B , 1998 Seismic activity and the criteria of seismic hazard assessment in the Ashgabat region, *Journal of Seismology* (submitted)

Karryev, B and Kanel, E , 1996 Contemporary seismicity of Turkmenistan, Presented at the Workshop NATO-ARW-951521 "Historical and Pre-historical Earthquakes", July 11-15, 1996, Erevan

Zaslavsky, Y , Karryev, B , Gitterman, Y , Esenov, E , Kanel, E and Shapira, A , 1998 Microzonation studies of Ashgabat, Turkmenistan, using microtremor measurements Presented at the XXVI General Assembly of the European Seismological Commission (ESC), Tel-Aviv, August 23-28, 1998

Kanel, E and Karryev, B , 1998 A fractal approach to recent seismicity analysis, Presented at the XXVI General Assembly of the European Seismological Commission (ESC), Tel-Aviv, August 23-28, 1998

## 6 PROJECT PRODUCTIVITY

The main product of our project is the seismic zonation map of Ashgabat and the associated earthquake hazard functions presented above These will hopefully serve as a basis for improving building regulations in Turkmenistan in general and in Ashgabat in particular The initial investigations we have performed on existing buildings yielded important information to be used for better assessment of the earthquake risk and expected loss due to earthquakes in the Ashgabat region

For reasons beyond our control, the high productivity of the project in its initial stages quickly decreased In many respects, we were rather lucky that we managed to complete the main tasks of the project, although with an unavoidable delay

## 7. FUTURE WORK

Both collaborating institutes and all the people who were intensely involved in the project are very interested in continuing their collaboration in the field of Seismology, pending the improvements of working conditions and finance We enjoyed working together, but there is still much to be done and we are optimistic

## 8. ACKNOWLEDGEMENTS

We are grateful to geologists Felix Fainberg and Boris Vatolin for significant assistance in the selection of sites for microtremor measurements, to technician Kakali Ishanliev for valuable assistance during field work in Ashgabat, and to Dr Sergei Izumov for fruitful discussions on the regional seismotectonics

## 9. LITERATURE CITED

Brune, J N , 1970 Tectonic stress and spectra of seismic shear waves from earthquakes, *J Geopys Res* , 75 4997-5009

Boore, D M , 1983 Stochastic simulation of high-frequency ground motions based on seismological models of the radiated spectra, *Bull Seism Soc Am* , 73 1865-1894

Boore, D M and Atkinson, G M , 1987 Stochastic prediction of ground motion and spectral response parameters at hard-rock sites in Eastern North America, *Bull Seism Soc Am* 77 440-467

Feldman, L , Jaradat, M and Shapira, A , 1998 Unification of the local magnitude scale for the East Mediterranean region, Abstracts of the XXVI General Assembly of the European Seismological Commission, Tel-Aviv, August 23-28 1998

Hanks, T C and Kanamori, H , 1979 A moment magnitude scale, *J Geoph Res*, 84, B5 2348-2350

Joyner, W B , 1977 A Fortran program for calculating nonlinear seismic response, U S Geological Survey, Open File Report No 77-671

Karryev, B S , 1998 Seismic phenomena and structure of seismic process in KopetDag region/ Moscow, IFZ,1992 43pp

Malitzky, A and Shapira, A , 1996 PC-based Seismic Data Processing Software Package, Version 2 0 – User's Manual, GII Report Z1/567/79(111)

Nafi, K S and Shapira, A , 1998 On local magnitude determinations in the South Pacific region, submitted to SAFE - Bulletin Seismological Association of the Far East

Shapira, A and Avirav, V , 1995 PC-SDA operation manual (Version 2 2) GII Report Z1/567/79(110B)

Shapira, A and van Eck, T , 1993 Synthetic uniform hazard site specific response spectrum, *Natural Hazard*, 8 201-205

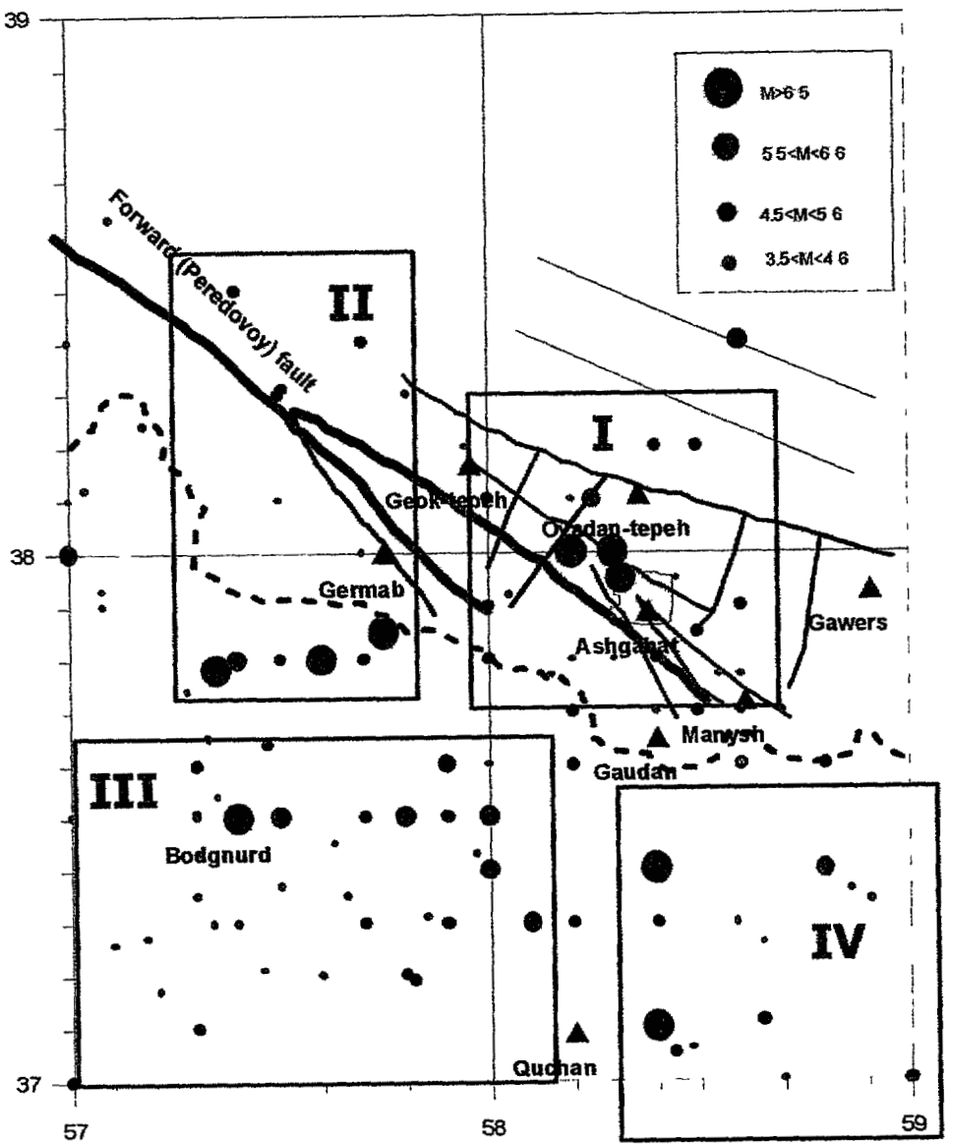


Figure 1 Map of earthquakes with M>3 5 (including historical) and four seismogenic zones determined in the Ashgabat region

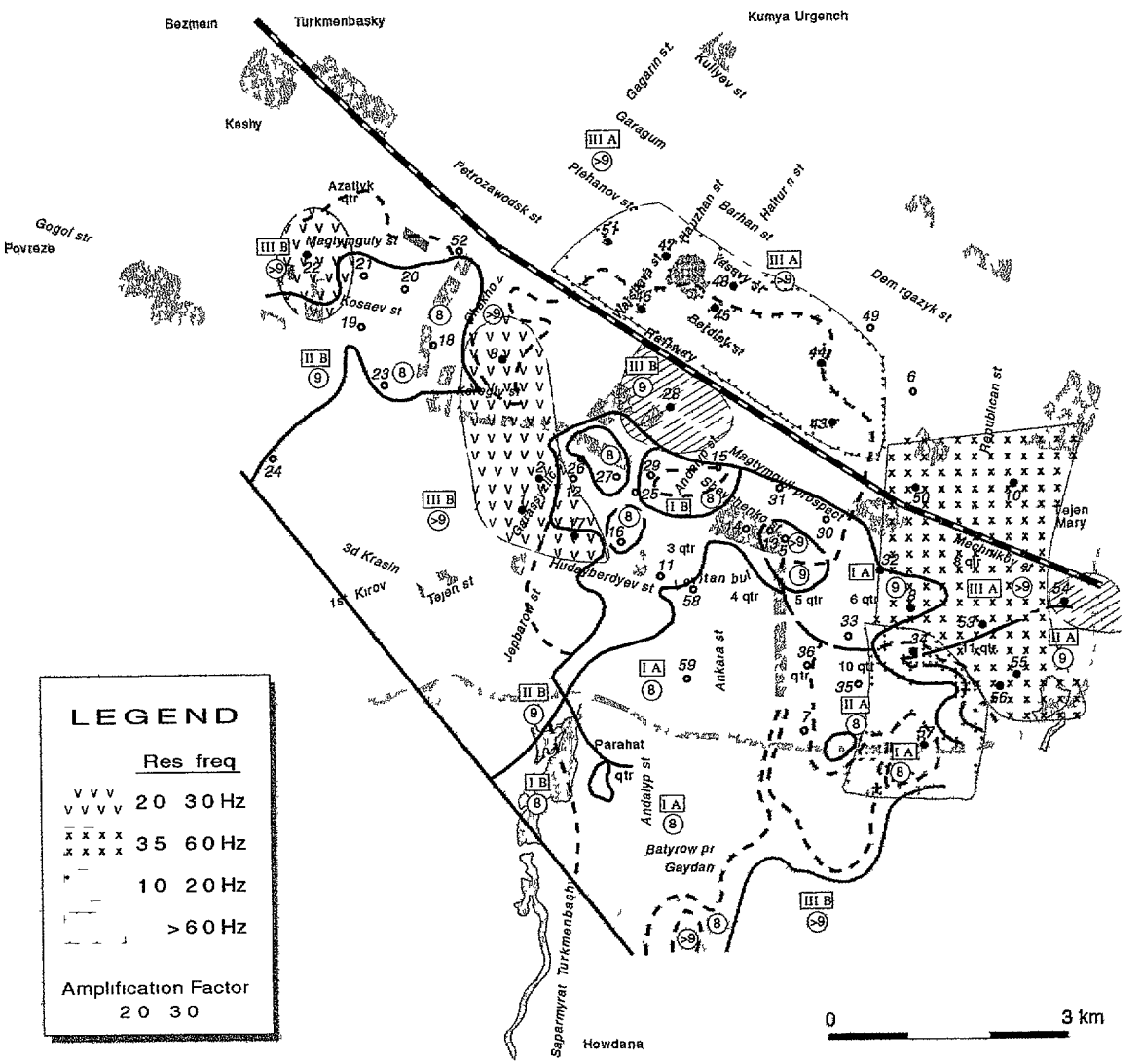


Figure 2 Distribution of fundamental frequencies estimated from H/V microtremor in Ashgabat

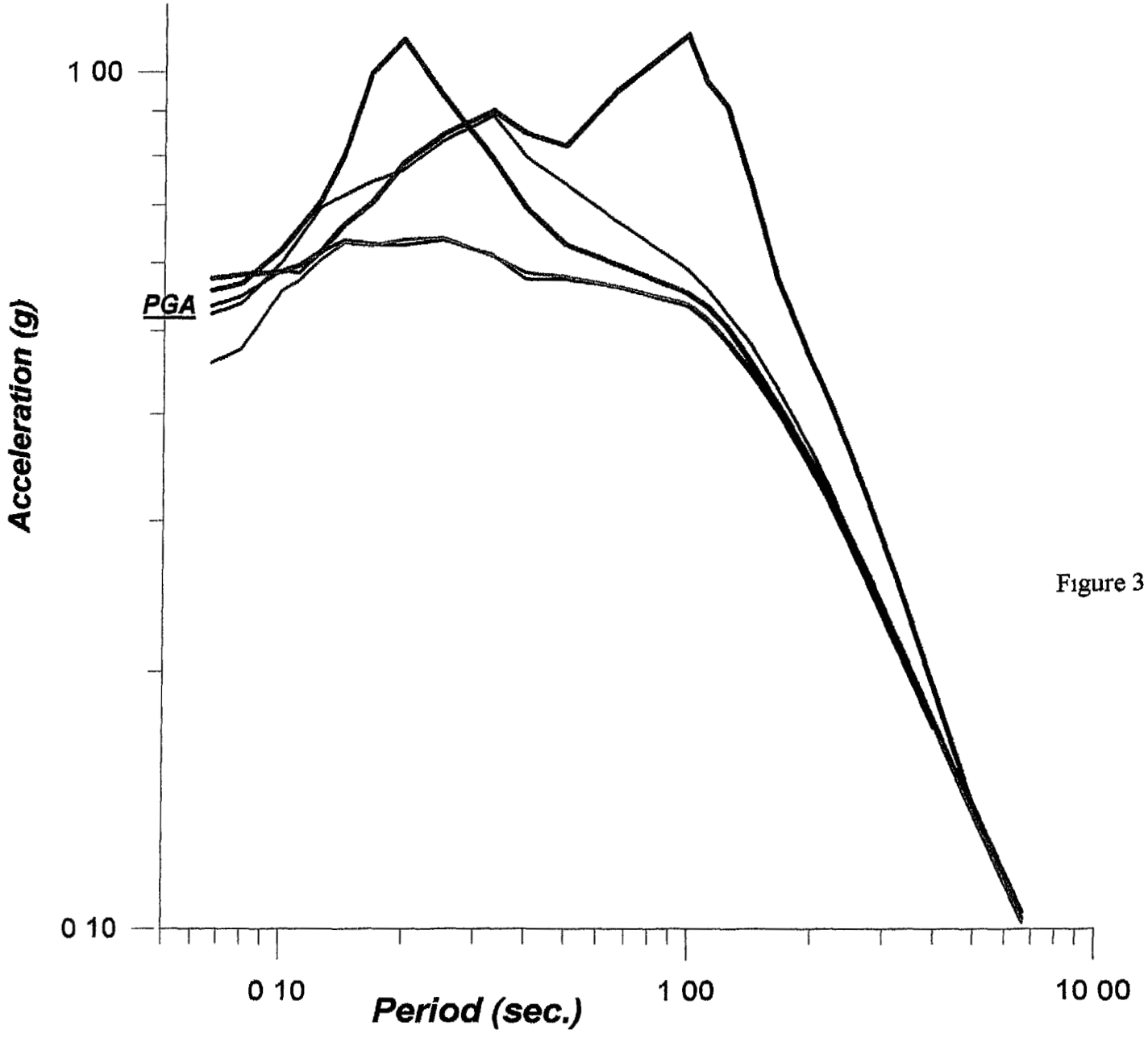


Figure 3 Uniform hazard acceleration spectra for the 4 seismic zones of Ashgabat

## Appendix A

# SEISMOTECTONICS AND SEISMICITY IN THE ASHGABAT REGION

## INTRODUCTION

The seismic activity in the central part of Kopetdag is associated with the dynamics of the interaction between the Turanian and Iranian plates and their formation at different ages The plates collide along the Kopetdag - Big Balhan deep fault Interpretation of geological data suggests that the Earth's crust at the Iranian platform is exposed to horizontal pressure that drives the mechanism of frequent earthquakes in this area (Myachkin, Lykov, 1983) The peculiarity of the regional field of compressive tectonic stresses lies in its horizontal component that is directed orthogonally to the Kopetdag deep fault The central part of this fault appears to be a right-lateral slip fault In the past millennia, strong earthquakes have repeatedly occurred in the Ashgabat region (Karryev, 1992, Karryev et al , 1994) and similar events will occur in the future This part of the project is focused on defining the seismogenic zones that pose the main threat to the Ashgabat urbanized area and quantifying the seismicity of those zones

## TECTONICS AND SEISMICITY IN THE ASHGABAT REGION

### *TECTONICS*

The last destructive earthquake of 1948 is the most extensively studied earthquake in the Ashgabat region Analysis of this earthquake shows that its occurrence is associated with the junction of two large structural complexes, namely the Karakum platform in the North, and the Kopetdag alpine geo-syncline area in the South The forward Kopetdag trough represents a transitional zone and is located between these two complexes The through appears to be a relatively narrow trough with an abrupt southern wing and a flat northern one It is filled with a thick Mesozoic-Cenozoic sedimentary mass, under which the Paleozoic crystal basement is located at a depth of 10-12 km The southern board of the trough is formed abruptly by the main Kopetdag deep fault expressed by a sub-surface thrust

Major seismic generating features of central Kopetdag are associated with the interaction of the Earth's crust segments within the main Kopetdag and Meshkhed-Kuchan deep fault zones The most intensive and contrasting movements are located in the north-west of Ashgabat (the towns of Bezmein and Geok-Tepeh) and the northern part of the Meshkhed-Kuchan depression

Seismic activity is also associated with the large diagonal shifts with surface expression of large basement splits that are also confirmed by the presence of thermal and mineral water

origins along them The largest and most active regions (in the neotectonic epoch) of diagonal faults are the Nokhur-Kazandzhik and Germab system of right up-thrown shifts, which can be traced from Kisil-Arvat to the Iranian territory, up to the Kuchan-Meshkhed depression and the Aselma upthrown-shift system (Aselma, Khalwat, Kharwar), joining with the Kopetdag fault to west-south-west from Ashgabat (see Fig A1)

The joint zone of diagonal shifts and the Kopetdag fault are characterized by morphological changes of local ruptures and creases, i e , up-thrown-shifts are sub-latitudinal oriented and they transform into the thrusts falling to the north Large joints with the Kopetdag fault are the locations of strong structural complication in the folded-ruptured picture of Central Kopetdag In these regions a forward Kopetdag trough structure is complicated by the existing fault that is buried under a sedimentary cover and a series of the most recent, wing-shaped sub-latitudinal creases (Kesheninbair and Pervomay anticlines)

Contrasting seismically active segments stand out over the whole length of the Germab fault system (on the region of Karkulab village, the town of Bodzhnurd in Northern Iran, etc ) Contrasting zones of seismic activity in Gaudan, Mannish and other local areas also characterize the Aselmin fault zone The groups of weak earthquakes are located close to Ashgabat, in the basement of the Keshennbair and Pervomay anticline creases in the Ashgabat region These areas were distinguished by the predominant grouping of aftershocks of the Ashgabat 1948 earthquake (Karryev, 1992)

In terms of macroseismicity, the largest concentration of relatively strong earthquakes is observed in the vicinity of the village of Germab (the Germab earthquakes of 1929, 1997), in the central part of the forward Kopetdag trough (to the west and south-east of Ashgabat) and in the Meshkhed-Kuchan trough (near Bodzhnurd and Kuchan) The most destructive earthquakes in the previous and present centuries took place in these zones (Karryev et al , 1994) A catalog of these events is given on floppy disk attached to this report The geological history of the Turkmen-Khorasan mountains shows that the earthquake in 1948 is related to the anomalous Ashgabat part of the trough The tectonic conditions of this region are stipulated by the lateral pressure on the forward Kopetdag trough in the direction from Kopetdag toward an Epiherzin platform The compression deformation in the trough results in soft mass pressure and brachy-anticline growth In the mountainous part, one can observe rocky mass (limestone) movements of thrust type complicated by shifts in the Kopetdag northern wing and other tectonic breakdowns of the upper structural floor, without pre-Alpine crystal basis catching

The pressure of the Kopetdag elevated to the north produces a concentration of maximum stresses in the boundary zone, namely in the Ashgabat part of the trough

Earthquakes seem to be the main form of this complicated relaxation process The peculiarities found when investigating the Ashgabat 1948 earthquake provide evidence of this (Rystanovich, 1967) The data for the aftershocks of this event show the diffusive character of their distribution and their location, 6-12 km deep The main aftershock concentration was observed to the northwest and southeast of Ashgabat

Determining the focal mechanism of the events has revealed compressive stresses perpendicular to the Kopetdag structure with an approximately horizontal rupture plane Macroseismic investigations in the source zone also coincide with movements of horizontal character Caves, falls or displacements most often occurred in a south or southeast direction Trains in Ashgabat and the Anew region were thrown off to the south from the roadbed On dry surface, the earthquake was expressed by cracks, different damages for cover sediments, by falls and landslides In Ashgabat the cracks could be measured in centimeters and the greatest number of cracks was observed southeast of Ashgabat The cracks commonly stretched along hills, in slopes or near foothills, Vertical displacements reached 1 m and the displacements were a few hundred meters in length Their appearance is mainly connected with the wide development of powerful loess-lime loam cover, yielding slightly to subsiding and slipping and a high level of soil water, this seems to provide the wide distribution of residual deformations in the surface layer Hence, the Ashgabat earthquake was not accompanied by apparently expressed ruptures that characterize tectonic earthquakes of similar scale except for the dislocations registered on the Aselma fault system (Poletaev, 1986) In the relatively non-deep location of the earthquake source, up to 10-15 km deep, the amplitude of the slip reduces rapidly towards the surface

The most probable source model of the catastrophic Ashgabat earthquake is associated with representing the development of a "blind inclined rupture" in contact with mass sedimentary rocks with a crystal basement surface (Rystanovich, 1967) Karryev et al (1994) reported that strong earthquakes occurred repeatedly in this territory during its history Although this region has been known from ancient times as an agricultural and commercial center, no historic monuments are preserved in the region The most ancient monument was a mosque in the Anew settlement (about 15 km east of Ashgabat) built in the middle of the XV century which was completely ruined by the 1948 earthquake This and similar information suggest that the repetition of earthquakes similar to the 1948 earthquake is no less than 500 years

According to archeological investigations, the direction of article falls and building construction displacements indicate the movements to the west and northwest in the earthquake source In the strike-slip reconstruction of the Nissah earthquake, performed by

A I Poletaev, horizontal right-shift displacement was determined to the southeast up to the region of the Pervomaisky settlement According to Rustanovich's representation, during the earthquake sedimentary rocks slipped from a pre-Alpine basement, about 1 5m to the north Conditions for similar rapid motion are predetermined by the tectonics of the Ashgabat region, i e by the tendency of the field of sub-meridian oriented tectonic forces to squeeze out the forward Kopetdag block The pressure deformation in the trough resulting in the Kesheninbair and Pervomaiski brachy-anticlines, cannot be compensated with pure neotectonic motion on the Aselma-Khalwat-Kharwar fault system Besides, the deformation exceeds the adhesion durability of sediment cover with the basement and resistance of the north elevated trough board This movement is accompanied by strike-slip along the Paleozoic basement and causes a destructive earthquake, mass rock balance loss and local displacements in the diagonal fault system compensating the loss of the trough stability

The stress relaxation following a destructive earthquake produces the observed diffusive aftershock activity and results in restoring the secular motion in the trough The block sub-horizontal slip evokes the occurrence of the tectonic motion in the Aselma diagonal faults system A similar model presentation of the 1948 earthquake makes it possible to distinguish some stages in the preparation of strong earthquakes in the Ashgabat region The first is associated with a long period of stress accumulation, sufficient for the seismic strike-slip of the trough At this stage a "deficit" of moderate earthquakes is accompanied by increasingly weak seismicity within structurally complicated zones, where the diagonal faults cross the Kopetdag fault The evidence of this can be seen in the regional seismic regime observed before and after the occurrence of the Ashgabat earthquake The time period necessary for starting the stability loss phase in the Ashgabat part of the trough may be estimated using the data on strong earthquake repetition in this region – it is, apparently, not less than 500-1000 years

A comparatively short interval for the preparation of a new earthquake source itself is connected with the breakdown of a secular motions course, seismic activation of peripheral sites, possible occurrence of moderate earthquakes in the diagonal fault system and in the northern trough Weakening is possible there through a series of tectonic motions From the data, the duration of this phase can be evaluated at 5-6 years A final phase is the strong earthquake occurrence resultong from the immediate slip of the local part of the trough and its displacement to the north A similar pattern of seismic dislocation distributions and tectonic movements was observed in 1948 At the same time the peculiar twisting of the block could occur with the elevation of its northwestern section and the lowering of its eastern section From the heterogeneous character of the building ruins and seismic dislocation distribution

observed, the tectonic motion played a considerable role The effect of seismic waves in the most intensive phase appeared to be influenced by specific local conditions The aftershock concentration in the northwestern zone, where a relative elevation was observed, seems to be the zone with the greatest stress concentration owing to the intrinsic increase of pressure in the rocks It could be suggested that the slip of the local section of the trough and the relaxation of its pressure deformation could occur as a series of strong and moderate earthquakes Many examples of similar seismic sequences in the last century have accumulated in the region, for example the Gazly strong earthquakes, the earthquake series in western Turkmenistan (Kumdag 1983, Burun 1984, Caspian 1986, 1989, etc ) No such information is available for the Ashgabat region, but in the seismic activation period of 500-1000 years the repetition interval of 5-10 years may be indistinguishable in a historic chronicle

*SEISMICITY*

The characteristics of source distribution in the Ashgabat region were obtained on the basis of the regional earthquake catalogues (Karryev et al , 1994) and the new data collected during this project Fig A2 shows the distribution of epicentral distances of earthquakes with M>4 from Ashgabat Most of these events are located within 100 km of Ashgabat Fig A3 depicts the epicenters of earthquakes with M>3 5 that occurred in the central part of Kopetdag Two main regions are distinguished One extends from Ashgabat to the northwest (the towns of Bezmein and Geok-Tepeh) and the other is located to the south of Ashgabat in Iran (the northern board of the Meshkhed-Kuchan depression along the Kuchan-Bodzhnurd road, parallel to the Kopetdag range) The main seismic hazard to Ashgabat is associated with activity in the first zone, where at least three strong earthquakes (M>7) and many earthquakes with less energy have occurred The Meshkhed-Kuchan depression zone is considerably less hazardous to Ashgabat Owing to the relatively large epicentral distances and significant attenuation of seismic energy propagating across the Kopetdag range, even strong earthquakes in this zone can cause damage only in the closest border regions of Turkmenistan For example, the strong earthquake of 1997 with M=7 was located in the epicentral zone of the destructive Germab 1929 earthquake and produced seismic intensities up to VI in the city of Ashgabat

The spatial distribution of seismicity is determined by the peculiarities of the regional tectonic structure The distribution of earthquake focal depths in central Kopetdag during the past 40 years is shown in Fig A4 Most events are located within the depth 10-15 km , probably close to the interface between the sediment mass rocks and the crystal basement

Based on instrumental data of seismic networks consisting of seven regional and nine portable stations in 1980-1990 and the currently operating network (5-6 stations), the peculiarities of the spatial distribution of earthquakes in the K>6 energy class were investigated for the time period 1980-1997 Three cross sections are shown in Fig A5

1 Profile 1-1 crosses the Ashgabat region from south to north A few zones with a higher concentration of events are located at depths of 5 and 10-15 km (up to the crystal basement of the Earth's crust)

2 Profile 2-2 passes from Manish to Germab It is characterized by the contrasting zone of events grouped within the 10 km range A zone of higher epicenter concentration is identified in the Ashgabat and Germab regions with a deepening in the region of the Bezmein sub-meridian fault

3 Profile 3-3 crosses the Bodzhnurd and Germab regions from south to north Its peculiarity appears to be the presence of hypocenter density cores at depths of 5-10 km in the Bodzhnurd earthquake zone and at a depth of 10 km in the focal area of Germab strong earthquakes (1929, 1997)

*RECURRENCE OF FELT EARTHQUAKES*

We evaluated the energy-frequency relationship per 200 years for Central Kopetdag $\log_{10}N = -0\ 45 \log_{10} E + 3\ 69$ The analysis of seismic intensities as a function of magnitude and distance (Fig A6) shows that the initial earthquake risk to Ashgabat ($I$=5) is formed by the cumulative effect of earthquakes with magnitudes 4 and higher at a distance of 5-150 km from the city It is composed of the contribution from the source zone of the strong Ashgabat earthquakes with magnitudes M=7 and above, which cause ground accelerations up to 0 45g and the contribution from the near source zone (up to 150 km) smaller earthquakes Fig A7 presents the data on seismic intensities in the city during the last 100 years This information was obtained from periodicals, eyewitness evidence and reports on the field investigations The figure also shows the expected intensities inferred from correlation between the intensity and local earthquake parameters (see Annual Report No 2) The differences between the observed and calculated intensity values are explained by the incomplete correspondence of the formula used and the real tectonic and physical conditions of the region and the source mechanism of individual earthquakes The remote earthquake effects evoking intensity up to $I$=3 can also cause calculated data omissions We have not included these in the regional earthquake catalogue Table A1 presents the average return periods of felt earthquakes in Ashgabat

**Table A1 - Felt Earthquakes in Ashgabat in the Past 100 Years (excluding aftershocks)**

| Intensity | 4 | 5 | 6 | 7 | 8 | 9 |
|---|---|---|---|---|---|---|
| Observed number of shocks | 30 | 15 | 7 | 4 | 1 | 1 |
| Calculated number of shocks | 34 | 18 | 8 | 4 | 1 | 1 |
| Return period (years) | 3 | 6 | 13 | 25 | >100 | >100 |

At least three catastrophic earthquakes are known to have occurred in Ashgabat in the last four thousand years This figure would yield an estimate of the return period of not less than 1000 years (assuming a stable seismic process) However, the recent example of the Germab active zone shows that seismic stability hypothesis can only serve as a very crude assessment, i e, the last strong earthquake in the Germab zone occurred in February 1997, with a magnitude of about 7, the previous event took place in 1929 A similar situation was also observed in the Kuchan earthquakes at the end of the last century, hence a conservative estimate of the return period of catastrophic earthquakes should be adopted in estimating the seismic hazard to Ashgabat

An approximate evaluation of strong earthquake manifestation in the city of Ashgabat is presented in Table A2

**Table A2 - First Approximation of Return Periods of Strong Earthquakes in the Ashgabat Seismic Zone**

| Magnitude | Return period, years |
|---|---|
| 5 | 15 ± 10 |
| 6 | 250 ± 50 |
| 7 | 1000 ± 500 |

## QUANTIFICATION OF THE SEISMICITY

We concentrated our efforts on the study of the self-similarity of two important aspects of the seismicity the variation of spatial and temporal distribution of the sources within the framework of the investigated region

### *SPATIAL DISTRIBUTION*

Many studies point out that most natural fractal phenomena are not uniform or symmetrical and, thus, the fractals of seismicity (i e spatial distributions of earthquakes) are similarly complicated It is not, therefore, sufficient to describe seismic activity by means of a

single dimension, but a multi-fractal dimension is more useful for comprehensive study of the heterogeneous fractals of earthquakes

The multi-fractal dimension Dq (i e , a generalized dimension) is a parameter which represents the complicated fractal structure of a multi-scaling nature Li et al (1994) proposed the extended G-P method, which can recover the dimension from a time series Its formula is

$$C_q(r) = \left\{ \frac{1}{N} \sum_{i}^{N} \left[ \sum_{\substack{j=1 \\ i \neq j}}^{N} \Theta(r - |X_i - X_j|) \right]^{q-1} \right\}^{\frac{1}{q-1}}$$

where Cq(r) is the *q*-th order correlation integral, $\Theta$ is a Heaviside step function, r is the scaling radius, N is the number of total earthquakes located within a research region in certain time interval, $X_i$ is the epicenter or hypocenter of the *I*-th event and $|X_i-X_j|$ is the distance

If the distribution of events is fractal then $C(r) \sim r^{Dq}$ and Dq=Ds is the spatial fractal dimension, we can evaluate the fractal dimension of a spatial distribution of earthquakes as the best fit slope of a straight line to the *log-log* plot of C(r) versus r Many Dq values can be calculated in the same way for other q values The curve of q -Dq is known as the *Dq spectra* We analyzed Dq-spectra for the same space distribution and found that N=400-500 to be the minimal value required for calculation Since the amount of available data for the Ashgabat area is insufficient, we had to use other methods in our investigations

The distribution of earthquake epicenters can be specified by describing how N events observed over a limited area are sorted to Q non-overlapping quadrates In case of the Polya-Eggenberger statistics (Korvin, 1992) the number of quadrates with *n* events is given by

$$P(n) = \frac{1}{n}\left[\frac{n}{Q}\right]^{n} (1+c)(1+2c) \quad (1+nc)\left\{1+\frac{cN}{Q}\right\}^{1/(c-n)}$$

where the coefficient C represents the degree of the event clustering Special cases of this equation are the Poisson distribution $P(n)=\exp(-\lambda)\lambda^n/n!$ for C=0, and the geometrical distribution $P(n)=n/(1+\lambda)^{n+1}$ for C=1, where $\lambda=N/Q$ When the value of C becomes large, P(n) approaches a power-lower distribution which is a characteristic of self-similar (fractal) clustering Thus, to study the clustering of earthquake we can divide the territory into grids of

equal area, count the number of events in each grid square and fit the distribution with the Polya model, assuming different values of C The most convenient way is to use the Morishita index (Aref'ev, Shebalin, 1988)

$$J_S = \frac{\sum_{i=1}^{Q} n_i(n_i - 1)}{N(N-1)}$$

where N is the total number of events, Q is the number of grids and $n_i$ is the number of events in the i-th grid

When the spatial distribution of earthquakes follows the P-E model, the Morishita index, J and the coefficient, C are related as J = C+1 In particular, J=1 for Poisson-random distribution, J>>1 for fractal clustering The Morishita index is easily computed and is also applicable when the epicenter distribution does not conform to the P-E model The Morishita index depends on grid size and, according to Ouchi and Uekawa (1986), this dependence is characteristically different for uniform and clustering distribution

The Morishita index for the earthquakes of the Ashgabat region was calculated The results for different energy classes show a considerable degree of clustering at all scale levels The degree of event clustering for short time intervals is much higher than for longer intervals, this suggests that there are small local zones with a high density of sources inside the limits of the Ashgabat region The temporal regime of activity in these zones is quite complicated (Kanel, 1990)

In recent years preliminary achievements have been made in the application of the fractal theory to earthquake research There are different approaches to the quantitative description of the spatial distribution of earthquakes, for example the box-counting algorithm (Sadovsky et al , 1984) and information fractal dimension (Zhu et al , 1993) We tested the methods in order to choose the most informative approach for studying the temporal variation of local seismicity and this would seem to be the *correlation integral method* proposed by Hirata et al (1987) The correlation integral of a distribution of N earthquakes is $C(r) = 2N_r/(N(N-1))$ where $N_r$ is the number of event pairs separated by a distance R less than r In this study we did not take into account the focal depth of the earthquake, hence the values of D are limited to the range from 0 (point) to 2 (uniform or random distribution without spatial grouping)

A critical issue in estimating the fractal dimension is the number of elements to be used There is no unique criterion prescribing the minimum of elements for fractal dimension

evaluations Several authors have addressed various aspects of this problem According to Smith (1988), the minimum number of elements to obtain a fractal dimension D with a quality Q (0<Q<1) is given by

$$N_{min} \geq \left( \frac{R(2-Q)}{2(1-Q)} \right)^{M}$$

where $R = r_{max}/ r_{min}$ and M is the integer part of the obtained fractal dimension Since we use only earthquake epicenters (owing to poor depth determination), we expect D to be less than 2 and, therefore, M=1 Setting Q=0 95 and R<15 for our zones, $N_{min}$ varies between 30 and 40

We derived an expression for the maximum value of D obtainable with a given number of data N Dmax=2log N/ log (Δ/r), where Δ is the largest distance in the data set Taking N=40 and Δ≤15r for our zones, we obtain a value $D_{max}$ = 2 7, which exceeds our estimates In this study we use the method of calculation fractal dimension D for catalog subsets with a fixed number of events (40 events - window with a shift of one event) We tested this approach on several subsets formed, with different energy thresholds, from the earthquake catalog all earthquakes with energy class K>10 5 (217 events), all earthquakes with K>8 5 (2100 events, earthquakes inside the 50 km radius circle from the Ashgabat city with K>8 5 from 1955 to 1997 (180 events) and others For each subset we plotted a *log C(r)-log(r)* relative curve and defined the best-fit slope of a straight line In the majority of cases, the correlation coefficient of points was larger than 0 96 We also tested different distance ranges for D calculations As shown in Table A3, the modification of the scaling region does not influence the temporal variation of the parameter

**Table A3 - Statistical Characteristics for Samples Taken from Background Seismicity**

| Spatial framework | Period | Number of events | Threshold energy class K | Scaling region (km) | $D_s$ mean value | Standard deviation |
|---|---|---|---|---|---|---|
| 37-39N 57-59E | 1955-1997 | 2100 | K>8 5 | 5 1 – 25 8 | 1 36 | 0 491 |
| | | | K>8 5 | 25 8 - 292 | 1 06 | 0 311 |
| 37-39N 57-59E | 1955-1997 | 638 | K>9 5 | 5 1 – 25 8 | 1 59 | 0 517 |
| | | | K>9 5 | 25 8 - 292 | 1 07 | 0 320 |
| 37-39N 57-59E | 1955-1997 | 217 | K>10 5 | 5 1 – 25 8 | 1 792 | 0 330 |
| | | | K>10 5 | 25 8 - 292 | 1 120 | 0 213 |
| 37-39N 57-59E | 1955-1968 | 418 | K>8 5 | 25 8 - 292 | 1 296 | 0 089 |
| | 1968-1979 | 598 | K>8 5 | 25 8 - 292 | 1 228 | 0 092 |
| | 1980-1990 | 530 | K>8 5 | 25 8 - 292 | 1 060 | 0 180 |
| | 1991-1996 | 283 | K>8 5 | 25 8 - 292 | 0 940 | 0 130 |
| 37-39N 57-59E | 1955-1970 | 120 | K>9 5 | 25 8 - 292 | 1 34 | 0 092 |
| | 1970-1979 | 128 | K>9 5 | 25 8 - 292 | 1 299 | 0 096 |
| | 1980-1990 | 130 | K>9 5 | 25 8 - 292 | 1 111 | 0 100 |
| | 1990-1996 | 104 | K>9 5 | 25 8 - 292 | 1 02 | 0 054 |
| 11 15 68 M5 6, R=50 | 1957-1996 | 180 | K>8 5 | 5 1 - 86 5 | 1 331 | 0 255 |
| 37-38N 57-58E | 1955-1996 | 1362 | K>8 5 | 11 4 - 128 | 1 345 | 0 292 |
| | 1955-1996 | 401 | K>9 5 | 11 4 - 128 | 1 332 | 0 293 |
| | 1955-1996 | 135 | K>10 5 | 11 4 - 128 | 1 430 | 0 216 |

It may be noted that a major shock is usually preceded by a maximum D value and followed by a minimum value Major shocks were defined as earthquakes whose energy class exceeds the threshold energy class for 4-5 units For the time intervals without a "main" shock, the fractal dimension demonstrated "quasi constant" behavior To check the possibility of "random effect" we simulated pseudo-random catalogs by changing the order of the occurrence of events Temporal variations of the spatial fractal dimensions calculated for the pseudo-random catalogs do not show any correlation with relatively strong events We also studied the influence of the earthquake location accuracy on the value of the spatial fractal dimension by simulating cases when a random error was added to the true location (within realistic boundaries) The D-values obtained by the simulations are quite close to those estimated for the real data The decrease of spatial fractal dimensions prior to large

earthquakes has also been reported by other researchers (Rossi, 1990, De Rubeis et al , 1993, Zhu et al , 1993) Table A4 shows the long-term values of spatial fractal dimensions $D_s$ for some regions calculated by all data that had been observed from 1955 to 1997

**Table A 4 – Long Term Spatial Fractal Dimensions**

| Space domain | Energy threshold | Number of events | Scaling region, km | $D_s$ |
|---|---|---|---|---|
| 37-39N 57-59E | K>8 5 | 2100 | 25 8 - 292 | 1 211 |
| 37-38N 57-58E | K>8 5 | 1362 | 11 4 - 128 | 1 570 |
| 37-39N 57-59E | K>9 5 | 638 | 25 8 - 292 | 1 160 |
| 37-38N 57-58E | K>9 5 | 401 | 11 4 - 128 | 1 527 |
| 37-39N 57-59E | K>10 5 | 217 | 25 8 - 292 | 1 156 |
| 37-38N 57-58E | K>10 5 | 135 | 11 4 - 128 | 1 509 |

The long term spatial fractal dimension for overall observations, including historical data, was estimated at $D_s$ = 1 48

## SEISMOGENIC ZONES AND THEIR FREQUENCY-K RELATIONSHIPS

The seismogenic zones that may affect Ashgabat are defined by combining the results of the fractal analysis of the earthquake catalog of Ashgabat, the historical evidence, the tectonic models for the region and the observed seismicity during the past 40 years Accordingly, we define the following four zones

1- Ashgabat

2- Germab

3- Bodgnurd

4- Quchan

The specified areas are shown in Fig A3 and Table A6 The list of the strongest earthquakes that occurred in each of these zones is presented in Table A5 The practice of earthquake monitoring in Turkmenistan is based on quantifying the earthquake strength in terms of Energy classes K According to Karryev (1992), an estimate of the $m_b$ magnitude is provided by the equation

$$m_b = (K - 2\ 7)/1\ 7 - 0\ 17$$

**Table A 5 - Largest Earthquakes Occurring in the Seismogenic Zones**

| Zones | Date | Latitude deg | Longitude deg. | Magnitude $m_b$ | Class K | Depth H, km |
|---|---|---|---|---|---|---|
| Ashgabat | 2000BC | 38 00 | 58 00 | 7 1 | 16 | 18 |
| | 10BC | 38 00 | 58 30 | 7 1 | 16 | 18 |
| | 1948 10 | 37 95 | 58 32 | 7 3 | 17 0 | 18 |
| | 1968 11 | 38 10 | 58 25 | 5 6 | 13 3 | 18 |
| Germab | 943 8 20 | 37 80 | 57 60 | 7 6 | 17 | 18 |
| | 1929 5 1 | 37 85 | 57 75 | 7 2 | 16 0 | 21 |
| | 1997 2 4 | 37 78 | 57 35 | 6 9 | 16 5 | 33 |
| Bodgnurd | 1810 | 38 00 | 57 00 | 6 5 | 15 | 11 |
| | 1833 | 37 30 | 58 10 | 6 2 | 15 | 14 |
| | 1879 4 2 | 37 50 | 57 40 | 6 7 | 16 | 15 |
| | 1902 1 31 | 37 40 | 58 00 | 6 2 | 15 2 | 10 |
| | 1948 6 18 | 37 50 | 57 80 | 5 9 | 15 | 15 |
| Quchan | 1831 6 | 36 80 | 58 40 | 6 9 | 16 | 29 |
| | 1851 6 | 36 80 | 58 40 | 6 9 | 16 | 15 |
| | 1871 12 | 37 40 | 58 40 | 7 2 | 16 5 | 28 |
| | 1872 1 | 37 10 | 58 40 | 6 3 | 15 0 | 15 |
| | 1895 1 | 37 10 | 58 40 | 6 0 | 15 0 | 20 |
| | 1948 10 | 37 40 | 58 80 | 6 0 | 15 | 12 |

Although the fractal analysis has revealed some temporal variations in the seismic activity, we concluded that, for long term seismic hazard assessment, we should adhere to the temporal distributions of earthquakes in accordance with the Guttenberg-Richter relationships which, in terms of Energy class K, have the forms of

$$\lg n = b_1*(K-8) + a_1 \quad \text{(A-1)}$$

$$\lg N = B*(K-8) + A \quad \text{(A-2)}$$

where n denotes the annual number of events of class K and N is the annual number of events with energy class K and higher

The best fit parameters for the four seismogenic zones are given in Table A6

## CONCLUSIONS

The results presented in this report summarize the most complete information currently available on the seismotectonics of the Ashgabat region and its seismicity In the framework of the US-AID project, this study has enabled us to define the main seismogenic zones that pose the seismic hazard to the city of Ashgabat and quantify the seismicity in each of them These results are summarized in Table A6 Based on this information it was then possible to simulate the expected seismicity around Ashgabat The simulations are integrated in the SvE computations for the assessment of the seismic hazard and risk to the city

**Table A6 - Seismogenic Zones in the Ashgabat Region**

| Seismogenic zones | Latitude, deg. | Longitude, deg | $a_1$ | $b_1$ | A | B | Depth, km | $D_s$ |
|---|---|---|---|---|---|---|---|---|
| Ashgabat | 37 35-38 30 | 58 00-58 70 | 2 32 | -0 46 | 2 52 | -0 48 | 10-20 | 1 52 |
| Germab | 37 70-38 60 | 57 30-57 75 | 2 79 | -0 46 | 3 01 | -0 48 | 5-10 | 1 38 |
| Bodgnurd | 37 00-37 65 | 57 00-58 15 | 3 11 | -0 47 | 3 37 | -0 49 | 5-10<br>40-50 | 1 59 |
| Quchan | 37 00-37 65 | 58 30-59 00 | 2 31 | -0 37 | 2 58 | -0 41 | 0-15<br>40-50 | 1 63 |

## REFERENCES


Aref'ev, S S and Shebalin, N V , 1988 Evaluation of Caucasus' earthquake clasterisation, Reports of the USSR Ac Sc , Vol 298 1349-1352

Hirata, T , Satoh, T and Ito, K , 1987 Fractal structure of spatial distribution of microfracturing in rocks, *Geoph J Royal Astr Soc* , 90, N2 369-374

De Rubeis, V , Dimitru, P , Papadimitriou, E and Tosi, P , 1993 Recurrent patterns in the spatial behavior of Italian seismicity revealed by the fractal approach, *Geoph Res Lett* , 133, 18 1911-1914

Kanel, E , 1990 Temporal structure peculiarities of the seismic process in the Ashkhabad seismoactive region, Inst Earth Phys , Moscow

Karryev, B S , 1992 Seismic phenomena and structure of seismic process in the KopetDag region/ Moscow, IFZ, 43pp

Karryev, B S , Ahmedova, S B and Golinsky, G L 1994 Powerful earthquakes in Turkmenistan/ Seismol Report of Turkmenistan -Ilim, N 2 21-48

Korvin, G , 1992 Fractal Models in the Earth Sciences, Elsiever Sc Pub , Amsterdam

Myachkin, V I and Lykov, V I, 1982 The main mechanism of the seimotectonic processes in South Turkmenistan and some experience of earthquake prediction, Dep VINITI, N47-82, 10p

Li, D, Zheng, Z and Wang, B, 1994 Research into the multi-fractals of earthquake spatial distribution, *Tectonophysics,* 233 91-97

Ouchi, T and Uekawa, T, 1986 Statistical analysis of the spatial distribution of earthquakes before and after large earthquakes, *Phys Earth Planet Int*, 44 211-255

Poletayev, A I, 1986 Seismotectonics of the Major Kopet Dagh Fault, Nauka, Moscow, 134 p

Rossi, G, 1990 Fractal dimension time variations in the Fruily (Nothern Italy) seismic area, *Boll Geof Teor Appl*, 32 175-183

Rustanovich, D N, 1967 Seismicity of the Turkmenistan territory and 1948 Ashkhabad Earthquake, *Voprosy Inzenernoy Seismologii*, v 12 Nauka, Moscow, 95p

Sadovskiy, M A, Golubeva, T V, Pisarenko, V F and Shnirman, M G, 1984 Characteristic dimensions of rock and hierarchical properties of seismicity *Izvestiya, Earth Phys*, 20 87-96

Smith, L A, 1988 Intrinsic limits of dimensional calculations *Phys Lett ,A*, 133(6) 283-288

Zhu, L-R, Zhou, S-Y, Wang, H-T, Bai, C-Y and Gong, Y-Q, 1993 Research on seismic information dimension, *Acta Seism Sinica*, 6, 1 19-27

## FIGURE CAPTIONS

Figure A1 - The fault tectonics of the Ashgabat area

a) Determined by structural geophysical studies and by morphological attributes the Forward Fault, the South-Forward fault, the North Ashkhabad fault, Izgant, Bezmein, Anew, Gawers,

b) Determined by structural geophysical studies the Ashkhabad fault, two un-named faults (4 and 5),

c) Determinated only by morphological attributes faults of the sedimentary cover Aselma (1), Khalwat (2), Kharwar (3)

Figure A2 - Distribution of epicentral distances from Ashgabat for earthquakes with M>4

Figure A3 - Map of earthquakes with M>3 5 (including historical) and four seismogenic zones determined in the Ashgabat region

Figure A4 - Earthquake depth distribution during the past 40 years for Central Kopetdag

Figure A5 - Profiles across seismic active regions

Figure A6 - Seismic intensity versus magnitude and distance for the Ashgabat region

Figure A7 - Observed seismic intensity for the city territory per last 100 years and corresponding calculated values

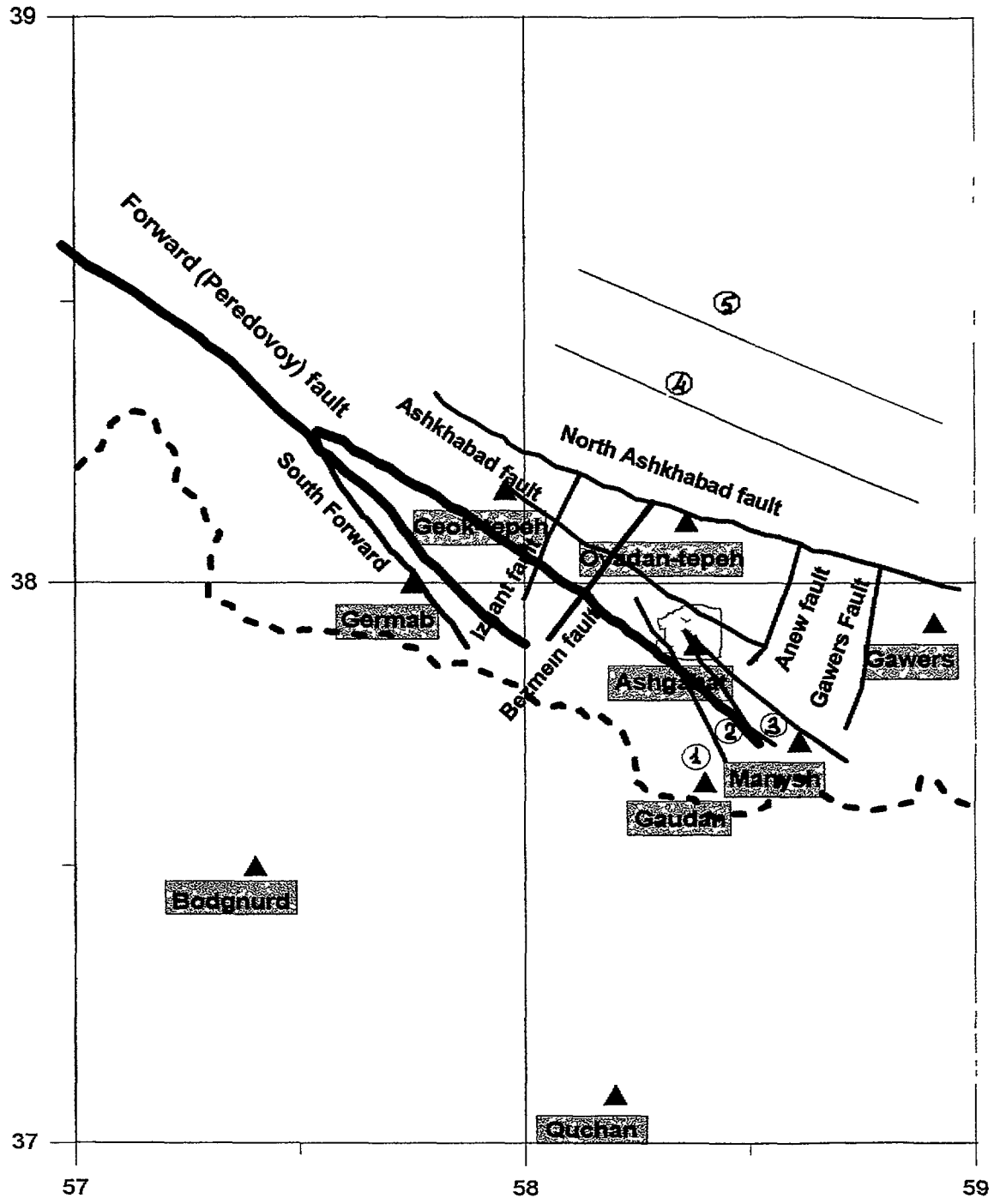


Figure A1 - The fault tectonics of the Ashgabat area

a) Determined by structural geophysical studies and by morphological attributes the Forward Fault, the South-Forward fault, the North Ashkhabad fault, Izgant, Bezmein, Anew, Gawers,

b) Determined by structural geophysical studies the Ashkhabad fault, two un-named faults (4 and 5),

c) Determinated only by morphological attributes faults of the sedimentary cover Aselma (1), Khalwat (2), Kharwar (3)

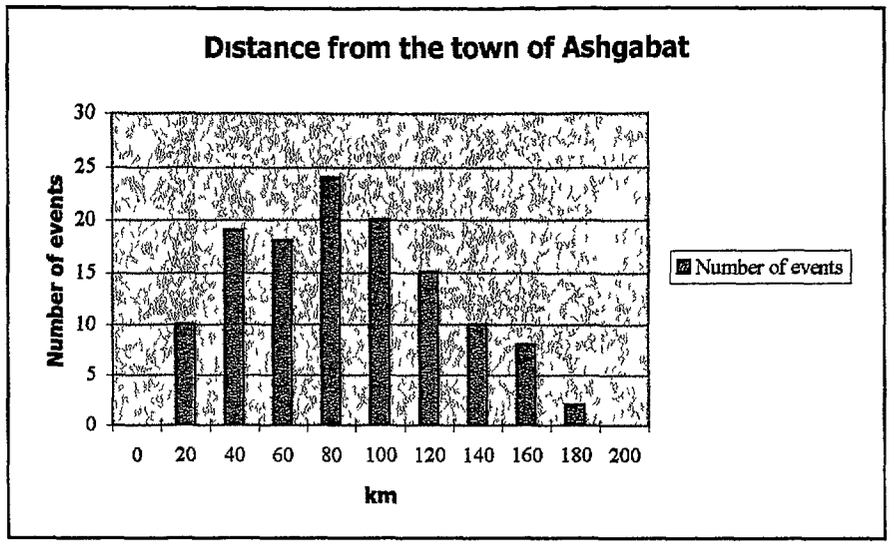


Figure A2 - Distribution of epicentral distances from Ashgabat for earthquakes with M>4

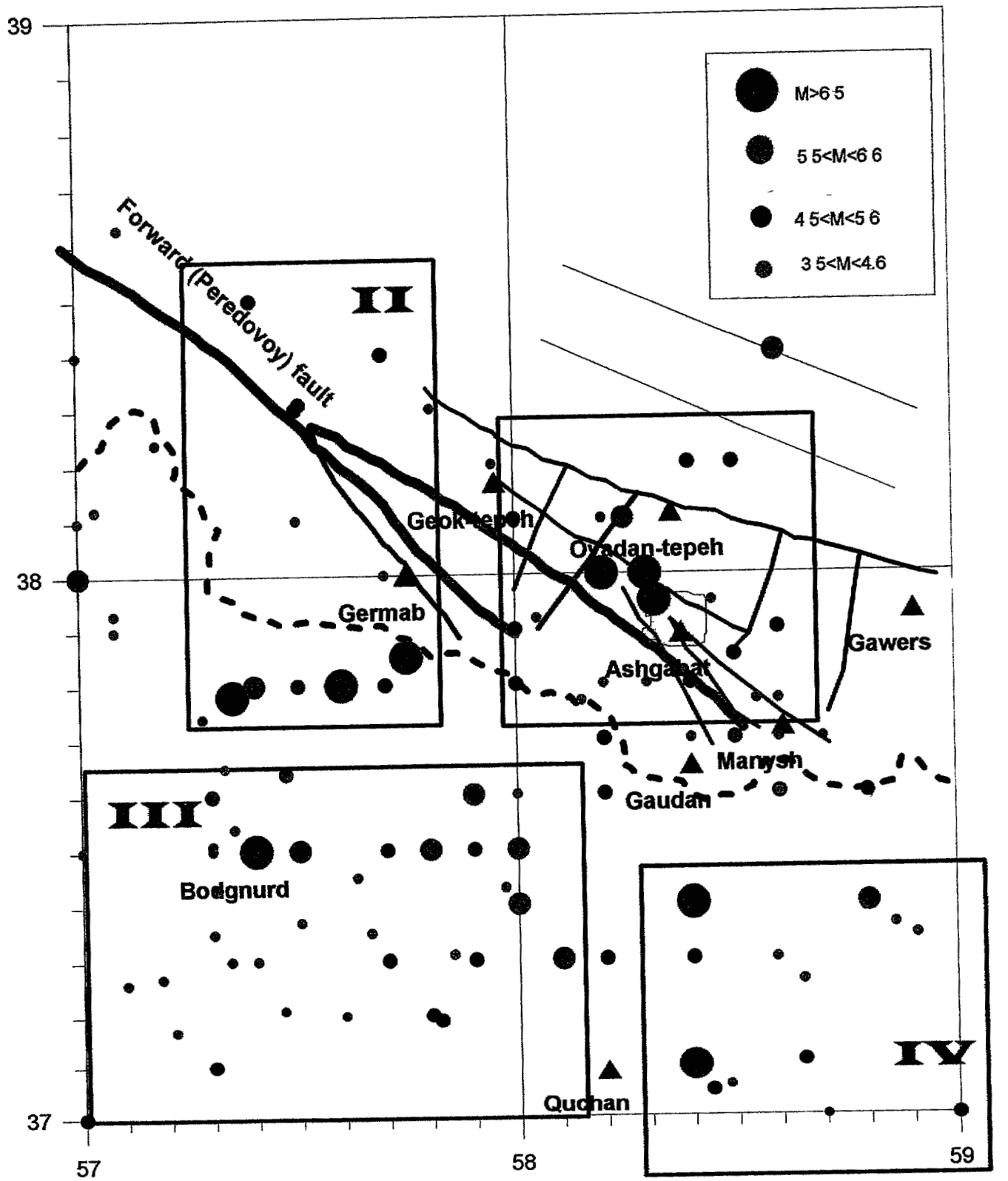


Figure A3 - Map of earthquakes with M>3 5 (including historical) and four seismogenic zones determined in the Ashgabat region

All evets within the region

| Energy Class/ Depth | 5 | 6 | 7 | 8 | 9 | 10 | 11 | 12 | 13 | 14 | 15 | |
|---|---|---|---|---|---|---|---|---|---|---|---|---|
| Not estimated | 3676 | 4162 | 3694 | 2611 | 819 | 185 | 47 | 20 | 0 | 0 | 0 | 15214 |
| 0<_h_< 5 | 84 | 294 | 505 | 493 | 343 | 122 | 40 | 8 | 0 | 1 | 0 | 1890 |
| 5<_h_<10 | 263 | 528 | 565 | 453 | 251 | 87 | 45 | 16 | 2 | 1 | 0 | 2211 |
| 10<_h_<15 | 117 | 290 | 315 | 207 | 75 | 22 | 12 | 5 | 5 | 0 | 0 | 1048 |
| 15<_h_<20 | 96 | 274 | 294 | 121 | 47 | 12 | 7 | 4 | 2 | 0 | 0 | 857 |
| 20<_h_<25 | 42 | 130 | 160 | 64 | 15 | 13 | 4 | 4 | 0 | 0 | 0 | 432 |
| 25<_h_<30 | 30 | 124 | 141 | 59 | 10 | 10 | 1 | 1 | 0 | 0 | 0 | 376 |
| 30<_h_<35 | 13 | 70 | 88 | 36 | 13 | 3 | 0 | 2 | 0 | 0 | 1 | 227 |
| 35<_h_<40 | 5 | 37 | 64 | 18 | 12 | 2 | 0 | 0 | 0 | 0 | 0 | 138 |
| 40<_h_<45 | 7 | 85 | 151 | 46 | 7 | 3 | 1 | 1 | 0 | 0 | 0 | 301 |
| 45<_h_<50 | 3 | 106 | 177 | 69 | 22 | 8 | 5 | 4 | 0 | 0 | 0 | 394 |
| 50<_h_<55 | 0 | 5 | 5 | 1 | 0 | 0 | 0 | 0 | 0 | 0 | 0 | 11 |
| Total | 4336 | 5106 | 6159 | 4178 | 1615 | 467 | 162 | 65 | 9 | 2 | 1 | 23099 |

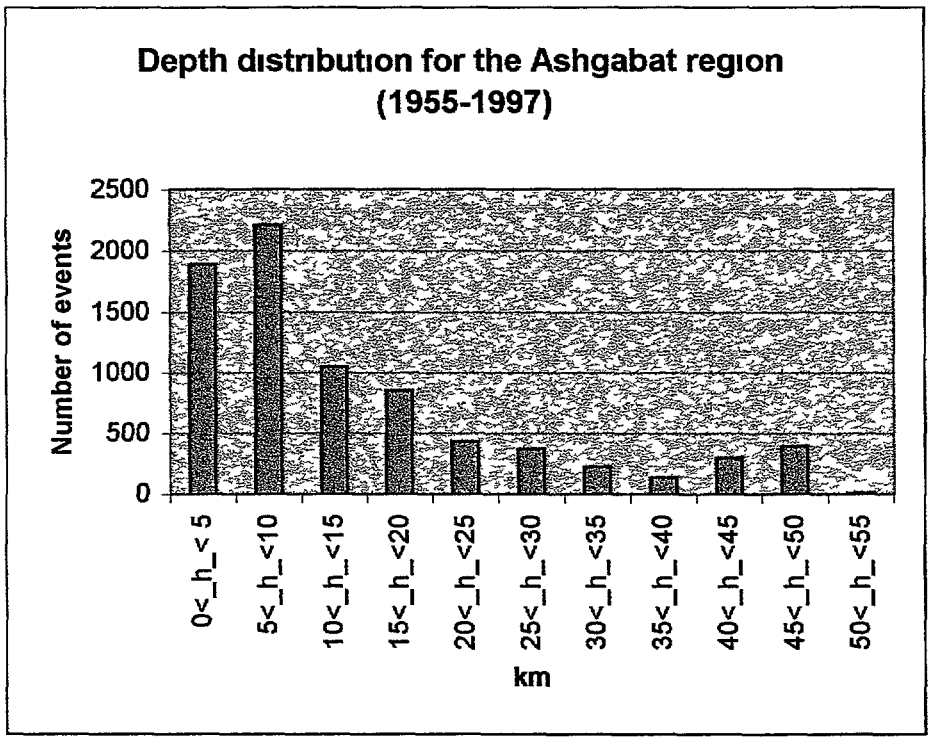


Figure A4 - Earthquake depth distribution during the past 40 years for Central Kopetdag

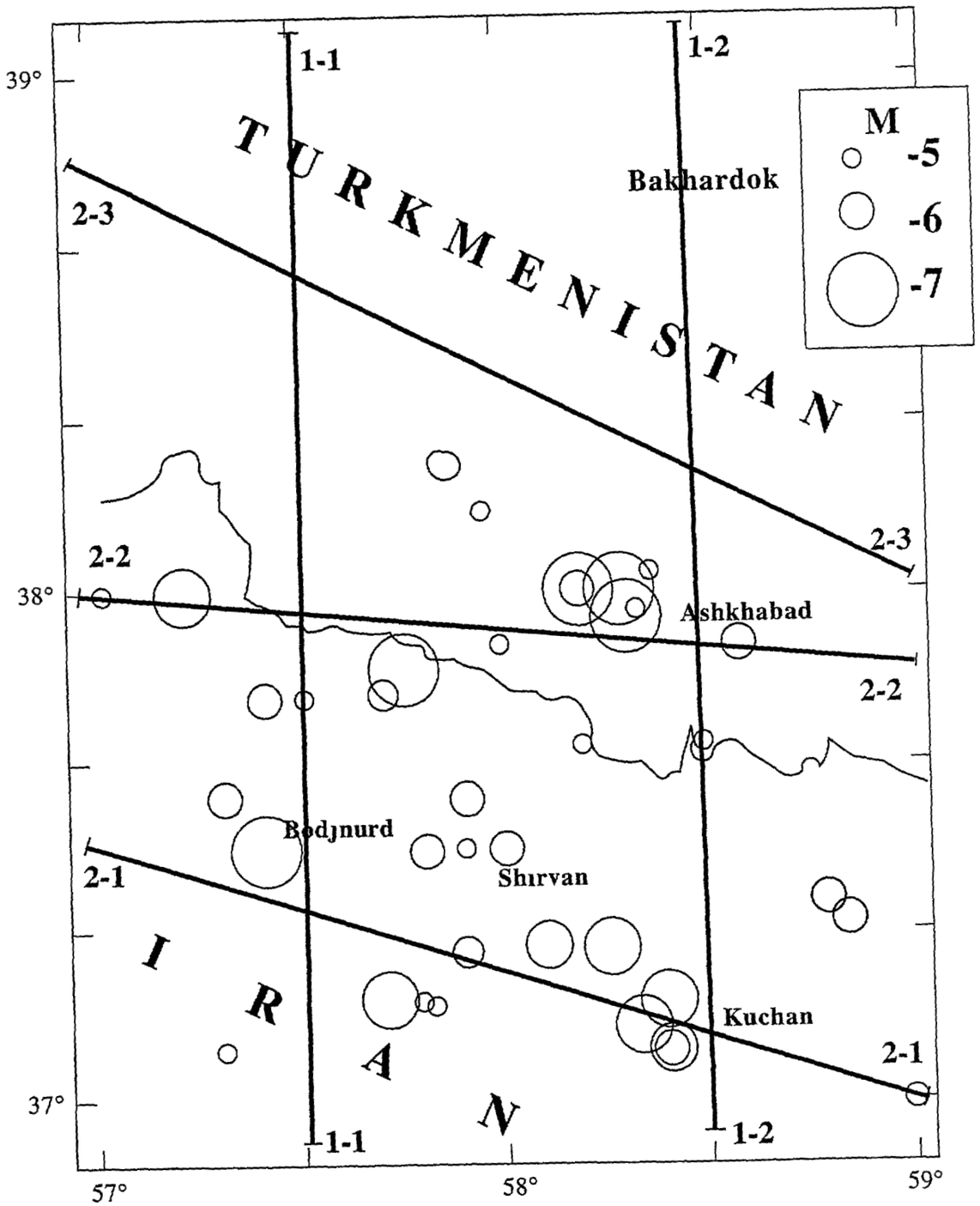


Figure A5 - Profiles across seismic active regions

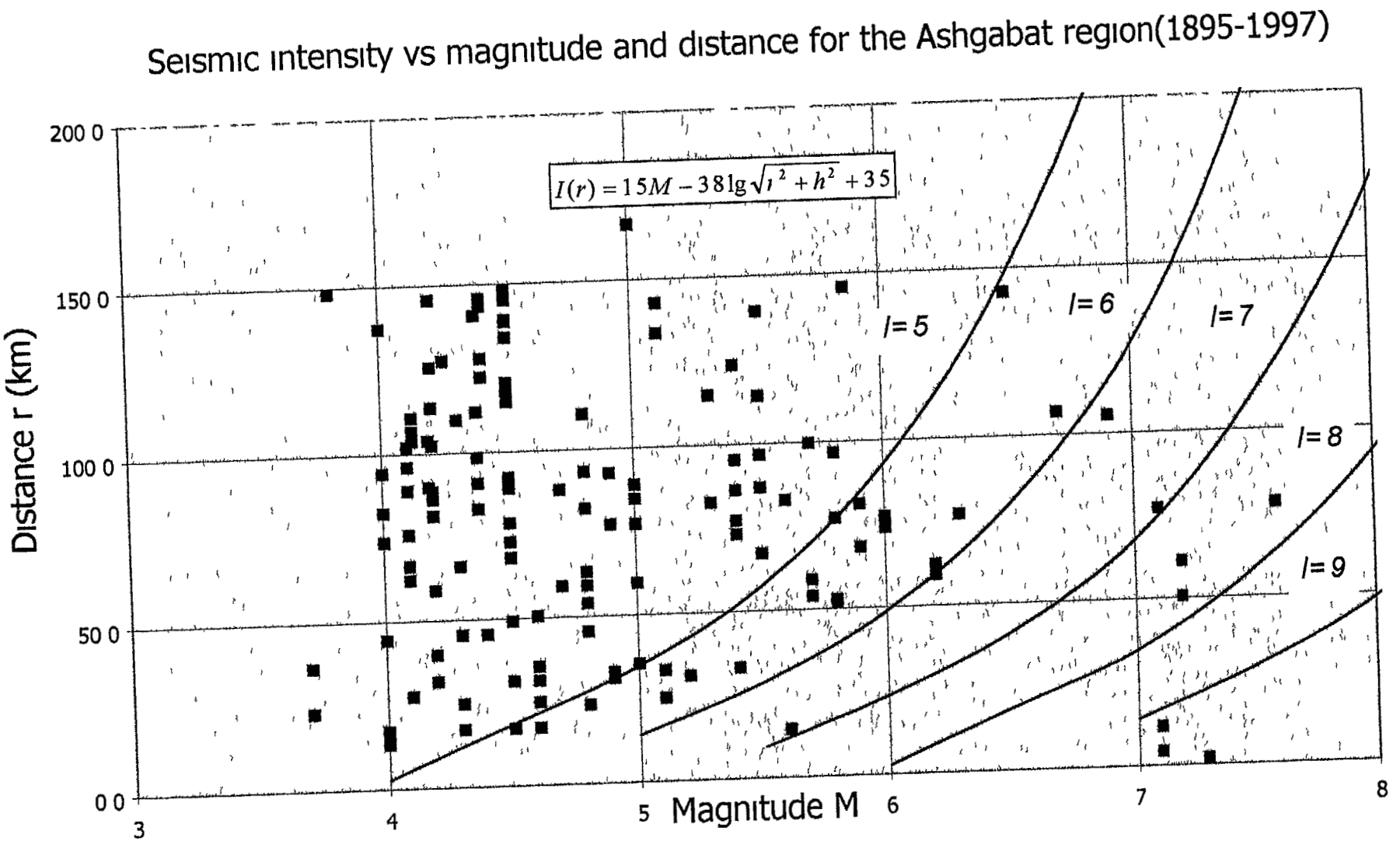


Figure A6 - Seismic intensity versus magnitude and distance for the Ashgabat region

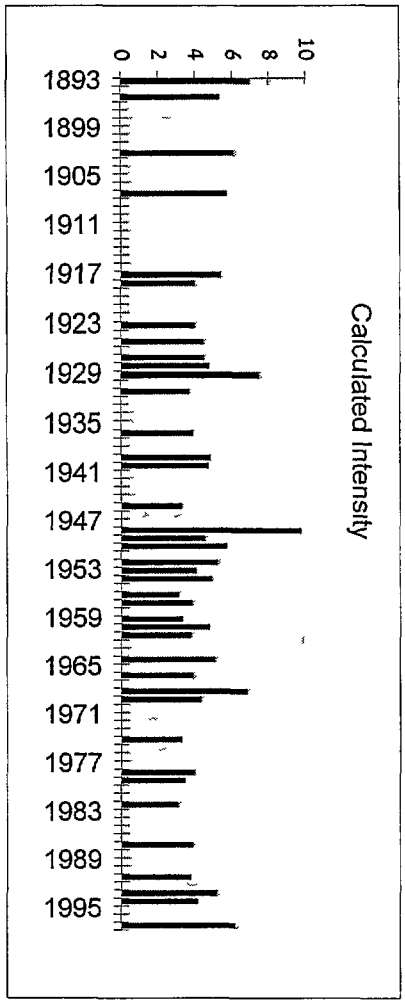


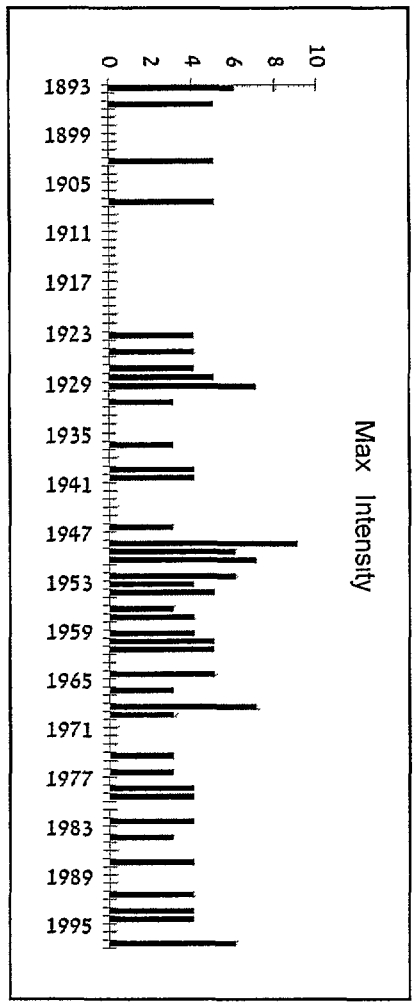


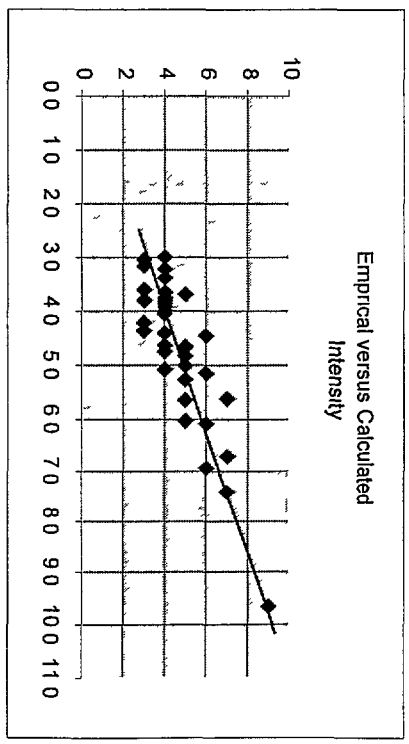


Figure A7 - Observed seismic intensity for the city territory per last 100 years and corresponding calculated values.

## Appendix B

# DATA ACQUISITION AT THE GEYOKCHA STATION AND ESTIMATION OF SOURCE PARAMETERS

In studying local and regional earthquakes to be used for evaluating their dynamic parameters, a permanent seismic station was installed at Geyokcha, near Ashgabat, through the joint efforts of both teams The station was tested, tuned and calibrated by Israeli specialists during their July 1996 visit At the outset the existing Russian SM-3 seismometers were used To improve maintenance, tuning, and data quality a set of new 3C L4C (Mark Products) seismometers were installed during the July 1997 visit by an Israel team

During the observation period the station recorded 18 earthquakes with magnitudes $m_b$ up to 3 8 which occurred in close proximity to Ashgabat The raw data (seismograms) and some source parameters were transferred through computer communications from SIBIS AST to GII The catalogue source parameters (origin time, coordinates and earthquake energetic class K) were estimated by the Turkmenian Complex Seismological Expedition (see Table B1) For one event (denoted by an asterisk) we found a discrepancy between the catalogue origin time and arrival time of seismic waves recorded in appropriate raw data files, therefore catalogue estimates (e g energy class K) for this event may be erroneous and actually relate to another event

**Table B1 - Seismic Events Recorded at the Geyokcha Station**

| # | Date | Origin time | Energy class K | Location | Distance (km) | Azimuth to event (°) |
|---|---|---|---|---|---|---|
| 1 | 96 07 12 | 09 46 25 | 6 5 | 37 91°N 58 31°E | 17 2 | 98 |
| 2 | 96 07 13 | 14 22 25 | 8 4 | 38 30°N 57 42°E | 73 6 | 304 |
| 3 | 96 07 13 | 19 32 13 | 4 0 | 37 90°N 57 90°E | 19 4 | 260 |
| 4 | 96 08 13 | 23 12 35 | 3 0 | 37 90°N 58 10°E | 3 4 | 180 |
| 5 | 96 08 18 | 04 25 38 | 7 0 | 37 90°N 58 10°E | 33 7 | 96 |
| 6 | 96 08 23 | 04 31 46 | 7 0 | 37 90°N 57 80°E | 28 5 | 263 |
| 7 | 96 09 27 | 20 36 08 | 6 2 | 37 99°N 57 82°E | 26 9 | 284 |
| 8 | 96 10 05 | 17 13 11 | 5 6 | 38 00°N 57 90°E | 20 6 | 292 |
| 9 | 97 07 10 | 13 14 51 | 9 6 | 37 40°N 57 50°E | 80 2 | 223 |

| # | Date | Origin time | Energy class K | Location | Distance (km) | Azimuth to event (°) |
|---|---|---|---|---|---|---|
| 10 | 97 07 11 | 13 45 42 | 7 0 | 37 60°N 57 40°E | 73 1 | 240 |
| 11 | 97 07 11 | 16 31 24 | 7 0 | 37 60°N 57 40°E | 73 1 | 240 |
| 12 | 97 07 11 | 16 47 01 | 8 0 | 37 80°N 57 30°E | 73 4 | 259 |
| 13 | 97 07 12 | 17 36 56 | 7 0 | 37 50°N 58 30°E | 50 4 | 161 |
| 14 | 97 07 12 | 19 44 09* | 7 0 | 37 60°N 57 40°E | 73 1 | 240 |
| 15 | 97 07 13 | 07 57 27 | 8 0 | 37 60°N 57 40°E | 73 1 | 240 |
| 16 | 97 07 13 | 18 13 24 | 8 0 | 37 90°N 57 50°E | 54 5 | 267 |
| 17 | 97 07 14 | 02 26 56 | 7 0 | 37 90°N 57 20°E | 80 8 | 268 |
| 18 | 97 07 14 | 08 49 06 | 8 0 | 37 80°N 57 60°E | 56 3 | 255 |

Based on this data we calculated the distance and azimuth to an event and also estimated source parameters of recorded earthquakes, presented in Table B2 The magnitude $m_b$ was calculated from the local relation (Karryev, 1992) $m_b = (K - 2\ 7)/1\ 7 - 0\ 17)$

**Table B2 - Source Parameters of Recorded Seismic Events**

| # | Date | Origin time | $m_b$ | Depth km | $W_o$, micron | Corner frequency $f_o$, (Hz) | Moment $M_o$, dyne*cm E+19 | Moment magnitude $M_m$ | Comments |
|---|---|---|---|---|---|---|---|---|---|
| 1 | 96 07 12 | 09 46 26 | 2 1 | 10 | 0 061 | 2 5 | 3 8 | 2 5 | strong clip |
| 2 | 96 07 13 | 14 22 28 | 3 18 | 9 | 0 131 | 2 0 | 24 0 | 2 99 | slight clip |
| 3 | 96 07 13 | 19 32 14 | 0 6 | 10 | 0 01 | 3 8 | 0 63 | 1 9 | - |
| 4 | 96 08 13 | 23 12 39 | 0 0 | 5 | 0 004 | 4 5 | 0 044 | 1 2 | - |
| 5 | 96 08 18 | 04 25 40 | 2 36 | 20 | 0 08 | 2 4 | 9 7 | 2 73 | strong clip |
| 6 | 96 08 23 | 04 31 48 | 2 36 | 5 | 0 066 | 2 5 | 6 4 | 2 6 | slight clip |
| 7 | 96 09 27 | 20 36 08 | 1 9 | 9 | 0 03 | 3 7 | 1 8 | 2 2 | - |
| 8 | 96 10 05 | 17 13 12 | 1 5 | 4 | 0 02 | 3 2 | 1 8 | 2 2 | - |
| 9 | 97 07 10 | 13 14 53 | 3 9 | 10 | 1 44 | 1 4 | 380 0 | 3 8 | slight clip |
| 10 | 97 07 11 | 13 45 48 | 2 36 | 10 | 0 09 | 2 4 | 19 0 | 2 92 | - |

| # | Date | Origin time | $m_b$ | Depth km | $W_o$, micron | Corner frequency $f_o$, (Hz) | Moment $M_o$, dyne*cm E+19 | Moment magnitude $M_m$ | Comments |
|---|---|---|---|---|---|---|---|---|---|
| 11 | 97 07 11 | 16 31 28 | 2 36 | 25 | 0 07 | 2 3 | 8 0 | 2 7 | - |
| 12 | 97 07 11 | 16 47 05 | 2 95 | 10 | 0 17 | 2 1 | 22 0 | 2 96 | - |
| 13 | 97 07 12 | 17 36 58 | 2 36 | 5 | 0 09 | 2 2 | 6 4 | 2 6 | - |
| 14 | 97 07 12 | 20 42 24 | 2 4 * | 10 | 0 13 | 2 9 | 27 0 | 3 02 | - |
| 15 | 97 07 13 | 07 57 31 | 2 95 | 19 | 0 15 | 2 0 | 29 0 | 3 04 | - |
| 16 | 97 07 13 | 18 13 26 | 2 95 | 10 | 0 37 | 2 0 | 64 0 | 3 3 | strong clip |
| 17 | 97 07 14 | 02 26 48 | 2 36 | 0 | 0 20 | 2 2 | 25 0 | 3 0 | - |
| 18 | 97 07 14 | 08 49 02 | 2 95 | 10 | 0 19 | 2 1 | 42 0 | 3 15 | - |

Depth and source estimates are obtained using PC-based GII-SDP (Seismic Data Processing) software developed and modified in the framework of this project by A Malitzky and A Shapira A local crust velocity model (see Table B3) was elaborated based on data for the Geyokcha area (Abaseev, 1991)

**Table B3 - Local Crust Model for the Kopet-Dag Area**

| Layer | Vp km/sec | Vs km/sec | Thickness km |
|---|---|---|---|
| 1 | 4 2 | 2 3 | 5 |
| 2 | 5 0 | 2 8 | 5 |
| 3 | 5 9 | 3 3 | 10 |
| 4 | 6 4 | 3 56 | 5 |
| 5 | 6 63 | 3 7 | 5 |
| 6 | 7 0 | 3 9 | 5 |
| 7 | 7 2 | 4 0 | 10 |
| 8 | 8 2 | 4 6 | - |

A high upper mantle P-wave velocity (8 2 km/sec) under station ABKT (in Geyokcha) was confirmed by data placed on the Web-site of the Synapse Center (McBride et al , 1998) The depth estimates obtained correspond well to long-time observations of local seismicity by Turkmenian seismologists, as shown on Fig A4 (Appendix A), which presents depth distribution of earthquakes for the Central Kopet-Dag region, based on the 1956-1996 catalogues completed during this project

## Appendix B



We evaluated flat spectral amplitude $\Omega$ and corner frequency $f_0$ from instrument corrected displacement spectra of S and S-coda waves (15-20 sec window) on vertical recording components and then calculated moment $M_0$ (see e g Brune, 1970)

$$M_0(\text{dyne*cm}) = k*4\pi\rho D\beta^3\Omega/CF$$

and moment magnitude $M_m$ (Hanks and Kanamori, 1979)

$$M_m = -10\ 6 + 0\ 6667*\lg(M_0)$$

where density $\rho$ =2 7 gr/cm$^3$, $\beta$=3 6 km/sec, C=2, F=0 18, k=1, D=R $^1$, R is the hypocentral distance in kms We applied the theoretical attenuation of spectral amplitude D=R $^1$, which was justified in this case by a satisfactory conformity of moment and body wave magnitude values (see Table B2) We also found a good correlation of energy class K estimations from local catalogues and moment magnitude $M_m$ values (see Fig B1)

$$M_m = 0\ 372*K + 0\ 152 \qquad \text{(B-1)}$$

Equation (B-1) was utilized for estimation coefficients of the magnitude-frequency relationship between incremental frequency *n* and moment magnitude $M_m$

$$\log n = a - b*M_m \qquad \text{(B-2)}$$

for the four seismogenic zones identified in the Ashgabat region presented in Chapter 3 1 and Appendix A (see Fig A3, Table A6), for which energy class - frequency equations (for a period of 42 years) were developed The coefficients (a, b) in Eq B-2 are presented in Table B4

**Table B4 - Coefficients of the Magnitude-Frequency Relationship for Selected Zones**

| Seismogenic zones | a | b |
|---|---|---|
| 1- Ashgabat | 6 18 | 1 235 |
| 2- Germab | 6 66 | 1 237 |
| 3- Bodgnurd | 7 03 | 1 254 |
| 4- Quchan | 5 41 | 0 993 |

Typical waveforms for the recorded earthquakes are presented in Figs B2 and B3 Low P/S amplitude ratios (less than 1) are observed for most events on all three components (see e g seismograms of the strongest event No 9 on Fig B2) The only exclusions are Events 3 and 7, where peak P-amplitude on vertical component exceeds S-amplitudes (Fig B3) Most events show the high-frequency content of seismic waves in the 3-10 Hz range, although Event 4 shows low-frequency S-waves (about 2 Hz) and very low frequency (0 5-1 0 Hz) surface waves are observed for Ev 13 (Fig B3)

## References

Abaseev, S S , 1991 Hypocenter evaluation for the 2D case (*in Russian*), Izv Academy of Science Turkmenian SSR, No 6

Brune, J N , 1970 Tectonic stress and spectra of seismic shear waves from earthquakes, *J Geopys Res*, 75 4997-5009

Hanks, T C and Kanamori, H , 1979 A moment magnitude scale, *J Geoph Res*, 84, B5 2348-2350

Karryev, B S , 1992 Seismic phenomena and structure of seismic process in the KopetDag region/ Moscow, IFZ, 43pp

McBride, J , Priestley, K and Rozhkov, M , 1998 Recent seismological projects and seismic investigations of the crust and upper mantle structure of the Caspian basin, SYNAPSE Science Center, Moscow, IRIS Data Analysis Center, Russia (http //home synapse ru/eng/products/caspian)

## FIGURE CAPTIONS

Fig B1 Experimental relationship between energy class K and moment magnitude $M_m$, based on records at the Geyokcha station

Fig B2 Typical waveforms of local earthquakes recorded at the Geyokcha station Low P/S (less than 1) amplitude ratios are observed at all three components

Fig B3 Examples of different waveforms of recorded earthquakes

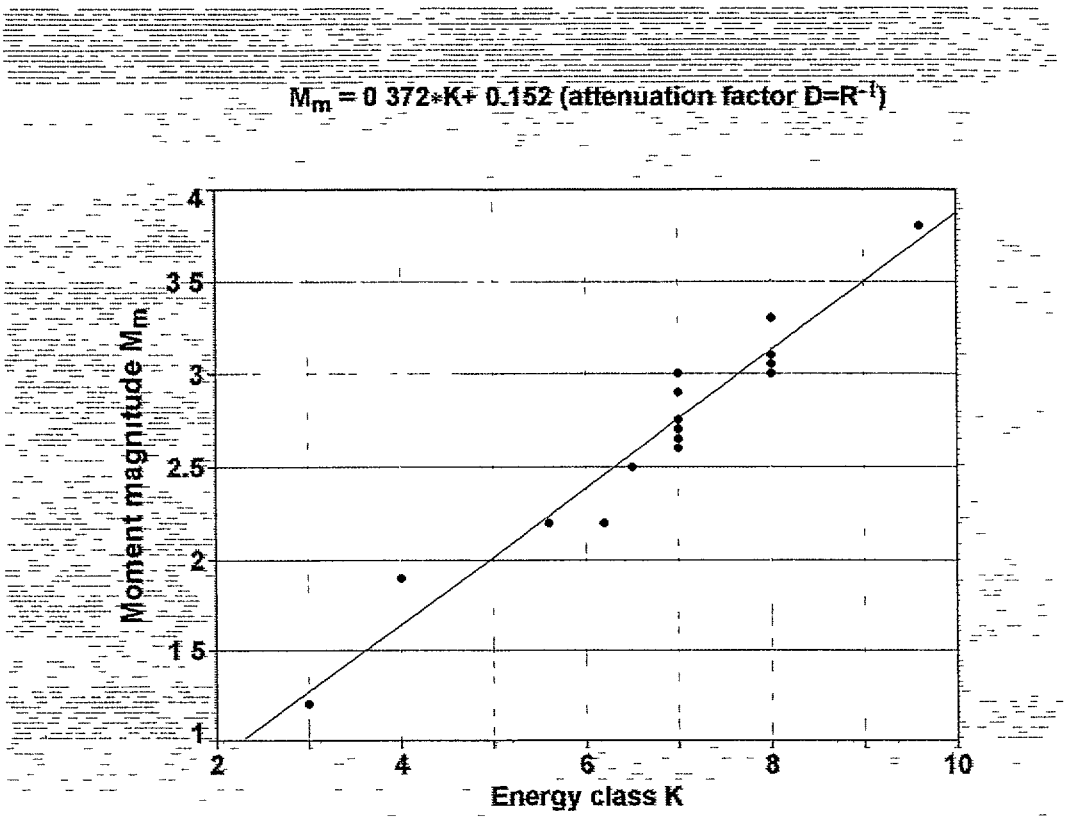


Figure B1 Experimental relationship between energy class K and moment magnitude $M_m$, based on records at the Geyokcha station

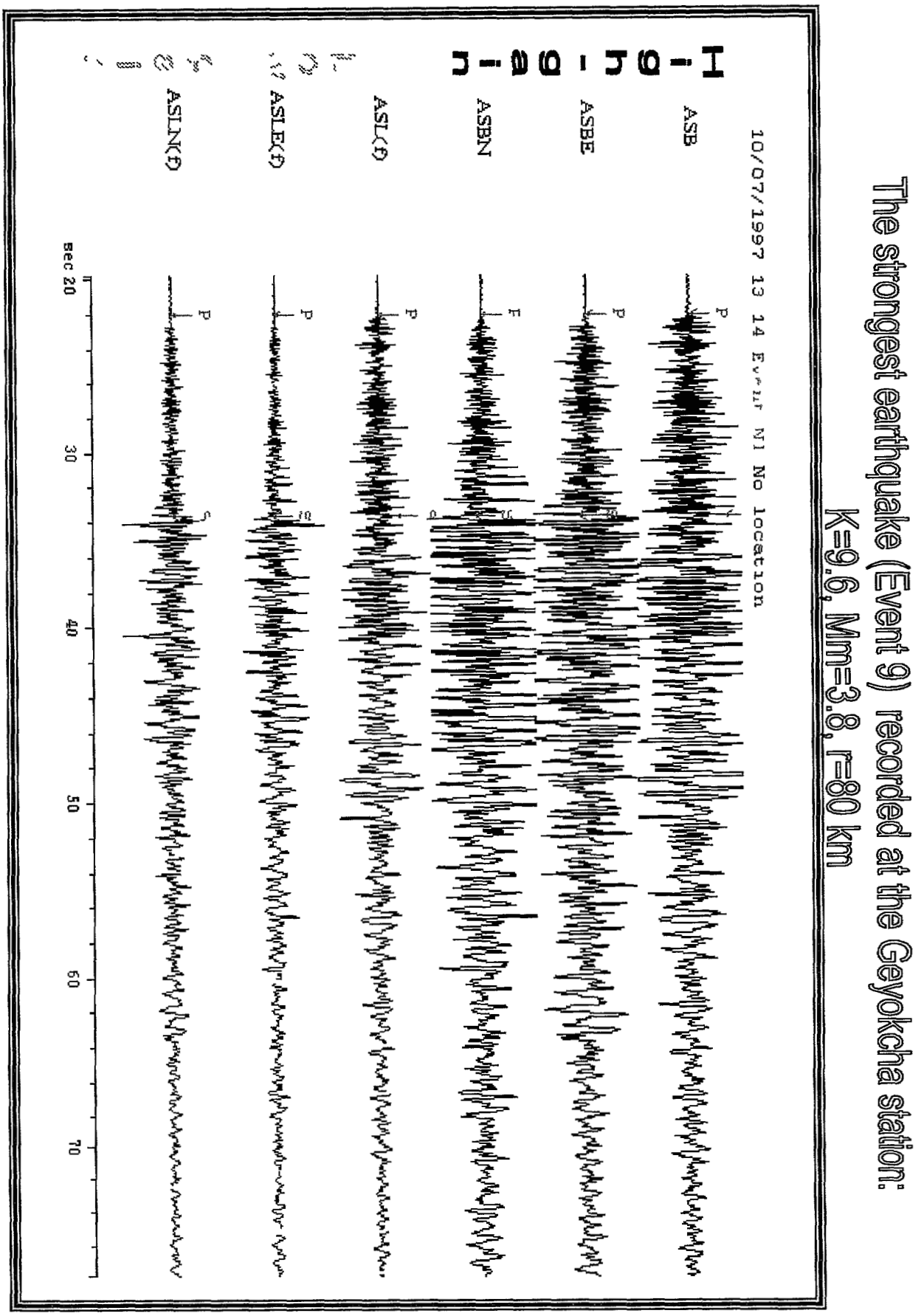


Figure B2 Typical waveforms of local earthquakes recorded at the Geyokcha station Low P/S (less than 1) amplitude ratios are observed at all three components

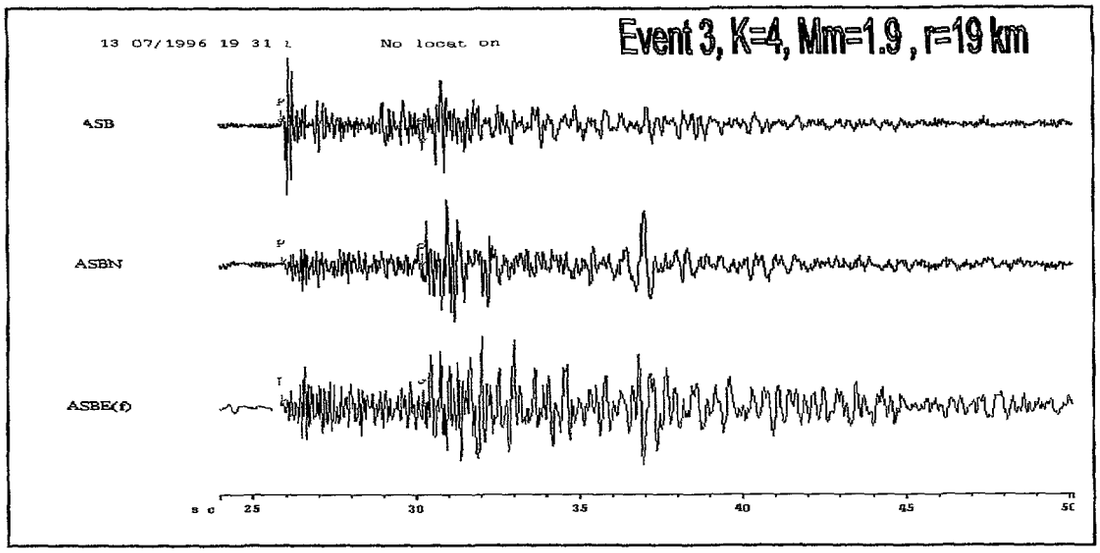


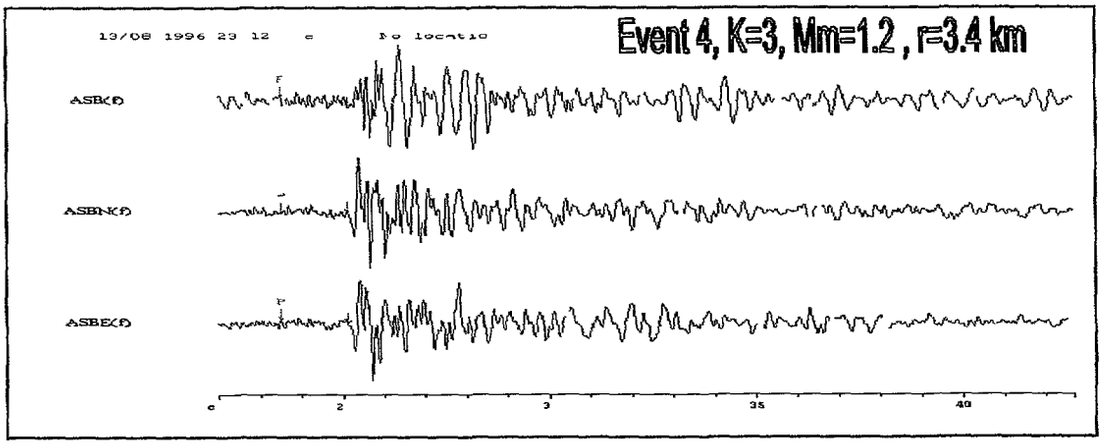


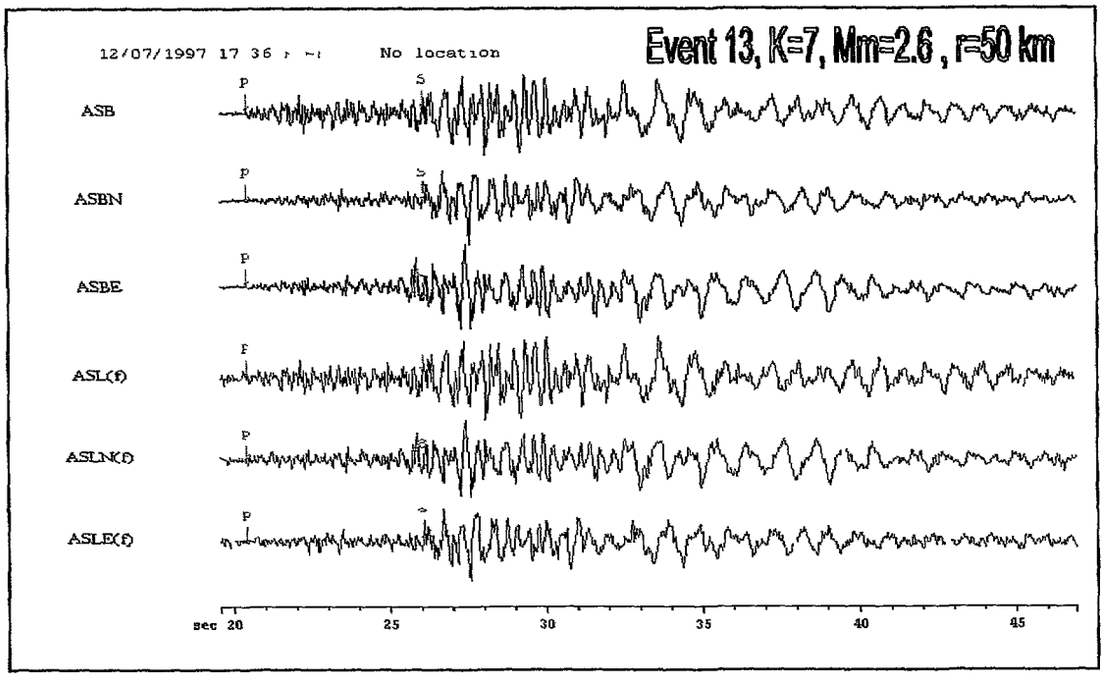


Figure B3 Examples of different waveforms of recorded earthquakes

Appendix C

# SITE EFFECT AND MICROZONATION IN ASHGABAT USING MICROTREMOR RECORDINGS

## INTRODUCTION

The great importance of site effects during earthquakes has been recognized since the early stages of seismology Resonance effects of the layers at the near-surface contribute heavily to the extent of loss and casualties during strong earthquakes A common factor in many of the methods for estimating amplification of the ground motions at a particular site due to its near-surface geology is to use a nearby bedrock site as the reference station These classic techniques for estimating site response depend on the availability of an adequate reference site The technique proposed by Nakamura (1989) has opened up fresh perspectives on site effect studies He hypothesized that site response could be estimated by dividing the horizontal noise spectrum ($H_s$) by the vertical noise spectrum ($V_s$) recorded at the same site

$$R_s(w)=|H_s(w)|/|V_s(w)|$$

This technique is used extensively around the globe (see,, for example, Ohmachi et al , 1991, Lermo and Chaves-Garsia, 1993, 1994, Field and Jacob, 1995, Zaslavsky et al , 1995, Gitterman at al , 1996, and others) The theoretical basis for this method was investigated by, for example, Field and Jacob (1993), Lachet and Bard (1994), Konno and Ohmachi (1998), Zaslavsky et al (1988) Although there are many unresolved questions regarding this technique, it is generally agreed that it does provide a reliable estimation of the fundamental resonance frequency of the upper layers of the site Ashgabat is characterized by a thick sedimentary basin that severely limits the application of other possible techniques for empirical determination of site response functions, consequently, the Nakamura method was used for microzoning of the Ashgabat area

## MEASUREMENTS

Ground motions (ambient noise) were recorded using the multi-channel, PC-based, digital seismic data acquisition system PC-SDA (Shapira and Avirav, 1995) developed by GII as part of the US-AID project One vertical and two horizontal seismometers (oriented north-south and east west) were installed at the investigated station The seismometers used

(L4C by Mark Products, USA) are sensitive velocity transducers with a natural frequency of 1 0 Hz and 70% critical damping Digital recordings with a sampling rate of 50 samples per second were made using 0 2-25 Hz band-pass filter

During the occupation of a site, we recorded three minutes of ground motions (seismic noise) every 15-20 minutes This was repeated six times to ensure accuracy Of the three minutes of microtremors recorded, from one to four 40 sec stationary segments were selected for analysis The signals were Fourier transformed using cosine tapering before transformation The spectra were then smoothed with a triangular moving Hanning window (0 4 Hz) and re-sampled every 0 024 Hz in the 0 5-10 Hz frequency range We computed the spectra for 10-16 non-overlapping 40 sec windows After calculating H/V ratios for all the time windows, the ratios were then arithmetically averaged to obtain a site-specific at each station During 1996 and 1997 we measured at 59 sites selected at random across Ashgabat The maps in Figs C1 and C2 show the locations of the investigated sites

## EMPIRICAL SITE RESPONSE EVALUATIONS

Ground motion amplifications were determined in terms of maximum Fourier velocity spectra and horizontal-to-vertical component spectral ratio Figs C3a and b show individual and average spectra of the horizontal components at Site 53 While the spectra show variation with time due to varying noise conditions, their shapes are similar These spectra are relatively flat between 0 5 and 2 Hz, but increase in amplitude near 4 Hz In Fig, C3c we present the average horizontal-to-vertical spectral ratios for this site (empirical transfer function) As shown, the empirical transfer functions has a predominant peak near 3 5 Hz The observed amplification factor is about 3 0

Examples of particle velocity spectra of the two horizontal components at Site 13 are presented in Figs C4a and b The solid lines represent the average Spectral levels of both components show an increase in seismic energy at about 4 Hz, however, the average horizontal-to-vertical spectral ratios (Fig C4c) are flat, suggesting no detectable amplification over the frequency range 0 5 to 10 Hz Figs C5a and b show the scatter of spectral ratios at different times of the day prevailing at Site 54 The spectral ratio curves also show (Fig C5c) a considerable amplification (a factor of about 3) at ~7 Hz Individual horizontal-to-vertical spectral ratios obtained from the recordings at Site 34 are shown in Fig C6 The spectral ratios are stable All of the ratios show a well-defined peak at about 5 Hz with an amplification factor of 2

Our measurements and spectral computations give credibility and reliability to the assumption that the observed spectral ratios are the true spectral presentations of the transfer function of the investigated sites The results are summarized in Tables C1, C2, and C3 As shown in these tables, we have specified certain zones within the city The geographical borders of these zones follow the observed macroseismic evidence quantified by the MSK intensity scale and coincide with the available geological and geotechnical data (Watolin and Esenov, 1984) The compiled geological, geotechnical and intensity data and the empirical site response determinations lead to the preparation of a zonation map that divides the town into four zones characterized by their fundamental resonance frequency Zone 1 – (1 0-2 0 Hz), Zone 2 – (2 0-3 0 Hz), Zone 3 – (3 5-6 0 Hz) and Zone 4 – (>6 0 Hz) The distribution of the predominant frequencies is shown in Figs C7 and C8 The open circles in these figures indicate those sites where predominant frequencies are not detectable by the data and the applied procedures At this stage we should note that our zonation map of Ashgabat is heavily influenced by the intensity and surface geology information In most cases we would avoid too high a dependence on historical evidence (intensities) since the intensities are themselves heavily dependent on the vulnerability of the buildings in the area affected by the earthquake In consultation with engineers in Ashgabat we were convinced that the differences in the engineering characteristics of the buildings during previous destructive earthquakes are only marginal and, therefore, the practical approach we adopted is reasonable

## Table C1

### Site Response Parameters in Areas where Intensities IX+ Have Been Observed

| Site No | Predominant frequency (Hz) | Site response | |
|---|---|---|---|
| | | Frequency (Hz) | Amplification |
| 4 | 3 0 | 3 0 | 3 0 |
| 22 | 2 0 | 5 0 | 3 0 |
| 53 | 4 0 | 3 5 | 3 0 |
| 54 | - | 7 0 | 3 0 |
| 1 | 0 9 | 1 0 | 2 5 |
| 47 | - | 3 3 | 2 5 |
| 2 | - | 2 0 | 2 0 |
| 3 | - | 2 5 | 2 0 |
| 10 | 4 0 | 2 0 | 2 0 |
| 48 | - | 3 5 | 2 0 |
| 50 | - | 2 0 | 2 0 |
| 51 | - | 3 5 | 2 0 |
| 5 | - | - | 1 0 |
| 6 | 4 0 | - | 1 0 |
| 13 | - | - | 1 0 |
| 24 | 2 8 | - | 1 0 |
| 49 | - | - | 1 0 |
| 52 | - | - | 1 0 |

## Table C2 - Site Response Parameters in Areas where Intensities IX Were Observed

| Site No | Predominant frequency (Hz) | Site response | |
|---|---|---|---|
| | | Frequency (Hz) | Amplification |
| 8 | 4 0 | 2 8 | 3 0 |
| 28 | - | 7 0 | 3 0 |
| 46 | - | 5 0 | 2 5 |
| 34 | - | 5 0 | 2 0 |
| 43 | - | 6 0 | 2 0 |
| 44 | - | 5 0 | 2 0 |
| 45 | - | 4 0 | 2 0 |
| 55 | - | 2 0 | 2 0 |
| 56 | - | 2 5 | 2 0 |
| 14 | - | - | 1 0 |
| 30 | - | - | 1 0 |
| 31 | 1 4 | - | 1 0 |
| 33 | - | - | 1 0 |
| 35 | - | - | 1 0 |

**Table C3**

**Site Response Parameters in Areas where Maximum Intensities VIII were Observed**

| Site No | Predominant frequency (Hz) | Site response | |
|---|---|---|---|
| | | Frequency (Hz) | Amplification |
| 57 | - | 5 5 | 3 1 |
| 41 | 2 0 | 2 0 | 2 0 |
| 42 | 1 8 | 1 5 | 2 0 |
| 17 | 1 8 | 1 8 | 1 8 |
| 37 | - | 1 0 | 1 8 |
| 38 | 1 2 | 1 0 | 1 8 |
| 7 | - | - | 1 0 |
| 9 | - | - | 1 0 |
| 11 | - | - | 1 0 |
| 12 | 8 0 | - | 1 0 |
| 15 | - | - | 1 0 |
| 16 | - | - | 1 0 |
| 18 | - | - | 1 0 |
| 19 | 3 0 | - | 1 0 |
| 20 | 1 5 | - | 1 0 |
| 21 | - | - | 1 0 |
| 23 | - | - | 1 0 |
| 25 | 1 8 | - | 1 0 |
| 26 | - | - | 1 0 |
| 27 | | | 1 0 |
| 29 | 1 8 | - | 1 0 |
| 32 | - | - | 1 0 |
| 36 | - | - | 1 0 |
| 39 | - | - | 1 0 |
| 40 | 2 0 | - | 1 0 |
| 58 | 3 0 | - | 1 0 |
| 59 | - | - | 1 0 |

## ANALYTICAL RESPONSE FUNCTIONS AND SUBSURFACE MODELS

The main goal of site response measurements is to provide a subsurface model that will, in turn, be implemented in analytical computations of the SvE for estimating the site response during strong earthquakes The shape of the empirical transfer functions determined in this study, as well as the good agreement between both horizontal components, strongly suggest that site effects in this region can be modeled by an 1D subsurface model The analytical site response determinations were made according to the Joyner method (1977) The computer code of Joyner (1977) requires an 1D model as input The relevant models for the different zones are derived from geological, geotechnical and seismic data collected in the area A typical example, based on drill-hole data, of a cross section of the city of Ashgabat is shown in Fig C9 The cross-section reveals interbedded layers of sand, clay and gravel The water table

is at or near the surface at many locations in Ashgabat The average shear-wave velocity, density and angle of internal friction were obtained from studies performed by Esenov (1989) These results are presented in Table C4

**Table C4 - Mechanical Properties of Different Materials in the Ashgabat Area**

| No | Material | P-wave (m/sec) | S-wave (m/sec) | Density (gr/sm$^3$) | Angle of internal friction (tg ) |
|---|---|---|---|---|---|
| 1 | Gravel and pebble | 850 | 500 | 1 8 | 40 |
| 2 | Interbedding of gravel and pebble with sandy loam and clay | 800 | 350 | 1 7 | 35 |
| 3 | Interbedding of sand and clay | 500 | 250 | 1 6 | 25 |
| 4 | Silt-stone | 1400-1800 | 700-900 | 2 0 | 42 |

The spread of the $V_s$ values measured for any given formation appears to be greater than 20% Likewise, layer thickness for the near surface sediments probably contains errors of at least 20% Any computation of site amplification based on such uncertain $V_s$ and thickness values is, therefore, subject to large errors which could exceed 50%, even for such an intensively surveyed area In the present study, the response functions are computed for linear behavior of the soils and were compared with the empirical functions By means of trial-and-error, the model parameters were adjusted (within a plausible range based on geological and geophysical data) to yield a better fit between the theoretical and the empirical assessments An example is shown in Figs C10a and b Table C5 shows the different subsurface models that provide a realistic assessment of the expected site effects across Ashgabat

**Table C5 - One-Dimensional Model Parameters Used for the Ashgabat Sites**

| Zone | Layer No | Thickness (m) | Density (gr/sm$^3$) | Shear-Wave (m/sec) |
|---|---|---|---|---|
| 1 | 1 | 10 | 1 6 | 250 |
| | 2 | 70 | 1 8 | 350 |
| | 3 | half space | 2 1 | 750 |
| 2 | 1 | 10 | 1 6 | 380 |
| | 2 | 35 | 1 8 | 500 |
| | 3 | half space | 2 0 | 900 |
| 3 | 1 | 10 | 1 6 | 250 |
| | 2 | 8 | 1 8 | 350 |
| | 3 | half space | 2 1 | 700 |
| 4 | 1 | 8 | 1 6 | 250 |
| | 2 | 4 | 1 8 | 350 |
| | 3 | half space | 2 1 | 700 |

## CONCLUSIONS

In this study, the effects of ground motion amplification due to local geology were evaluated for Ashgabat by analyzing microtremor records of 59 sites The spectral ratio between horizontal and vertical components (H/V ratio) has been used to estimate fundamental periods and amplification factors of site The predominant frequencies range from 1 to 7 Hz with amplification factor up to 3 Based on these results, the following conclusions can be drawn

1 The distribution of predominant frequencies across Ashgabat shows a correlation with surface geology information

2 Use of the Nakamura technique provides stable results for many, but not at all, sites This technique can provide good estimates not only of the ground natural frequency, but also of the corresponding spectral amplification To reach a better agreement between experimental data from microtremors and the microzonation map of Ashgabat, it is necessary to obtain recordings of earthquakes at several sites within the city

3 In site specific design spectra estimation 1D soil response approximation under non-linear conditions may provide valuable information A subsurface model based on geophysical and geological data may be over simplified presentation of the real conditions The empirical seismological evaluations of the site response are fundamentally more reliable

## REFERENCES

Esenov, E M , 1989 Regarding estimation of seismic risk of soils Ashgabad, Izv AC Turkmenistan, Ser FTN and GN, No 4, 14-19

Field, E N and Jacob, K N , 1993 The theoretical response of sedimentary layers to ambient seismic noise, *Geophysical Research Letters*, Vol 20, No 24 2925-2928

Field, E N and Jacob, K N , 1995 A comparison and test of various site-response estimation techniques including three that are not reference-site dependent, *Bull Seism Soc Am* 85 1127-1143

Gitterman, Y , Zaslavsky, Y , Shapira, A , and Shtivelman, V , 1996 Empirical site response evaluations case studies in Israel, *Soil Dynamics and Earthquake Engineering*, 15 447-463

Joyner, W B , 1977 A Fortran program for calculating nonlinear seismic response, U S Geological Survey, Open File Report 77-671

Konno, K and Ohmachi, T , 1998 Ground-motion characteristics estimated from spectral ratio between horizontal and vertical components of microtremors, *Bull Seism Soc Am* , 88 228-241

Lachet, C and Bard, P Y , 1994 Numerical and theoretical investigations on the possibilities and limitations of Nakamura's technique, *J Phys Earth*, 42 377-397

Lermo, J and Chaves-Garsia, F I , 1993 Site effect evaluation using spectral ratio with only one station, *Bull Seim Soc Am* , 83 1574-1594

Nakamura, Y , 1989 A method for dynamic characteristics estimation of the subsurface using microtremors on the ground surface, QR of RTRI, Vol 30, No 1, 25-23

Ohmachi, T , Nakamura, Y and Toshinawa, T , 1991 Ground motion characteristics of the San Francisco Bay area detected by microtremor measurements, Proceedings Second International Conference on Recent Advances in Geotechnical Earthquake Engineering and Soil Dynamics, Louis, Missouri, 1643-1648

Shapira, A and van Eck, T , 1993 Synthetic uniform hazard site specific response spectrum, *Natural Hazard*, 8, No 3, 217-226

Shapira, A , and Avirav, V , 1995 PC-SDA operational Manual, IPRG Rep No Z1/567/79

Watolin, B S and Esenov, E M , 1984 Map of microzonation in Ashgabat

Zaslavsky, Y , Shapira, A and Gitterman, Y , 1995 Site response estimations in Israel using weak motion measurements, Proceedings, 5th International Conference on Seismic Zonation, Nice, France, 1713-1722

Zaslavsky, Y , Shapira, A and Arzi, A A , 1998 Site response study in the Dead Sea area using earthquake end microtremors data, Proceeding of XXVI General Assembly of the European Seismological Commission (ESC), Tel Aviv, Israel, August 23-28, 258-262

# FIGURE CAPTIONS

Figure C1 Seismic microzonation map of Ashgabat with locations of recording sites

Figure C2 Seismic microzonation map of hotel area in Ashgabat with locations of recording sites

Figure C3 Time change of horizontal spectrum of microtremors recorded at Site 53 (a) for NS component, (b) for EW component and (c) average horizontal-to-vertical spectral ratios

Figure C4 Time change of horizontal spectrum of microtremors recorded at Site 13 (a) for NS component, (b) for EW component and (c) average horizontal-to-vertical spectral ratios

Figure C5 Time change of horizontal spectrum of microtremors recorded at Site 54 (a) for NS component, (b) for EW component and (c) average horizontal-to-vertical spectral ratios

Figure C6 Individual and average spectral ratios (NS and EW components) obtained from microtremors observed at Site 34

Figure C7 Example of geological cross-section for deposits of Ashgabat

Figure C8 Distribution of fundamental frequencies estimated from H/V ratio of microtremors in Ashgabat

Figure C9 Distribution of fundamental frequencies estimated from H/V ratio of microtremors at Hotel area in Ashgabat

Figure C10 Comparison of site response estimates obtained at Zones 2 and 4 average empirical transfer functions (thin line) and theoretical transfer function (heavy line) computed for model with two layers over a half-space

Fig 1 Seismic microzonation map of Ashgabat with locations recording sites

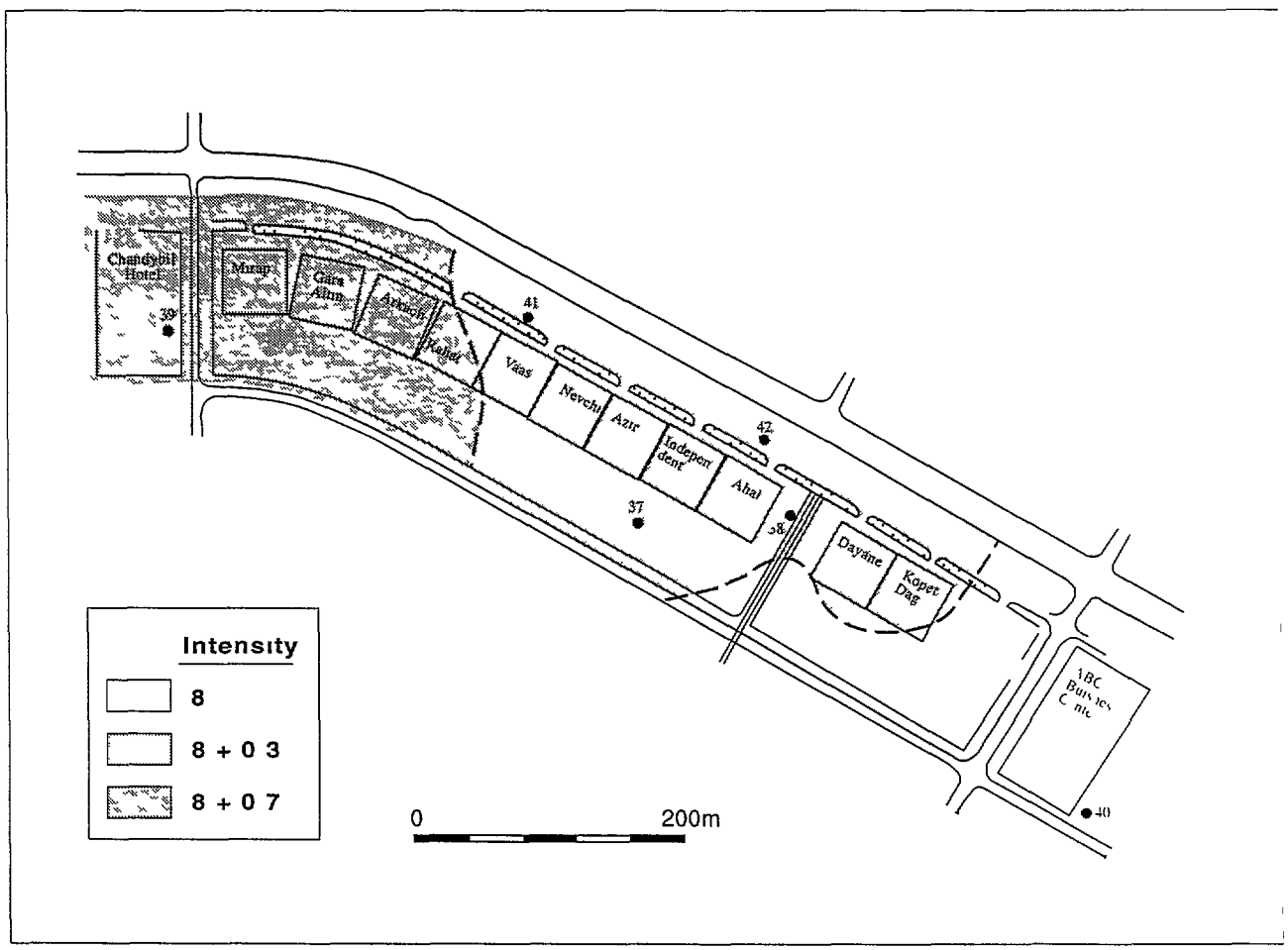


Figure C2 Seismic microzonation map of hotel area in Ashgabat with locations of recording sites

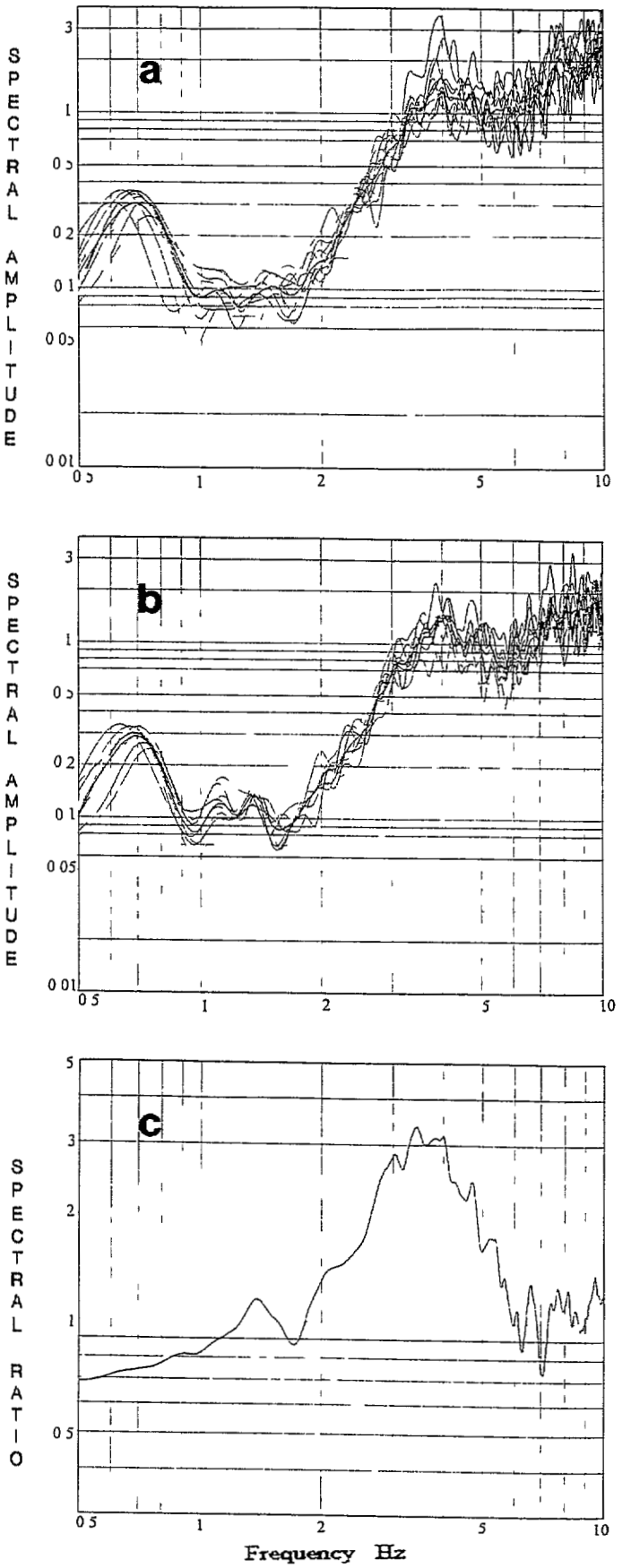


Figure C3 Time change of horizontal spectrum of microtremors recorded at Site 53 (a) for NS component, (b) for EW component and (c) average horizontal-to-vertical spectral ratios

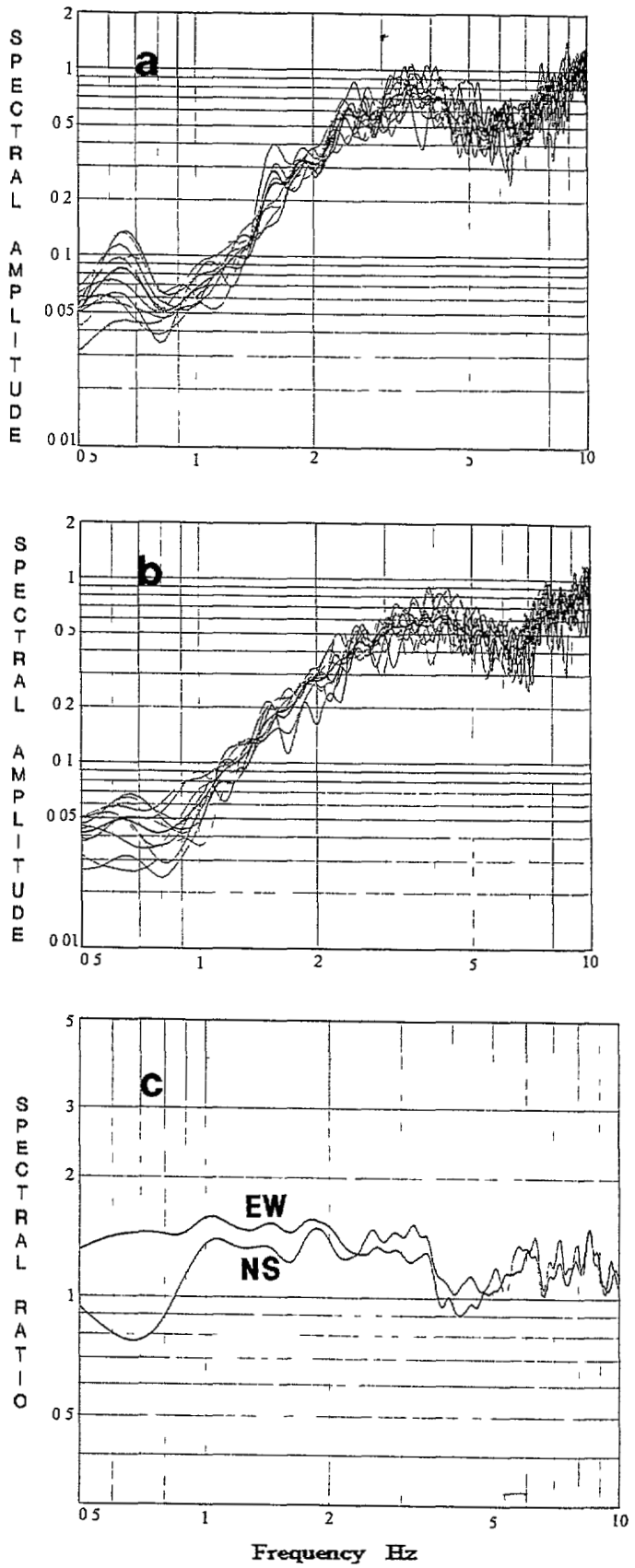


Figure C4 Time change of horizontal spectrum of microtremors recorded at Site 13 (a) for NS component, (b) for EW component and (c) average horizontal-to-vertical spectral ratios

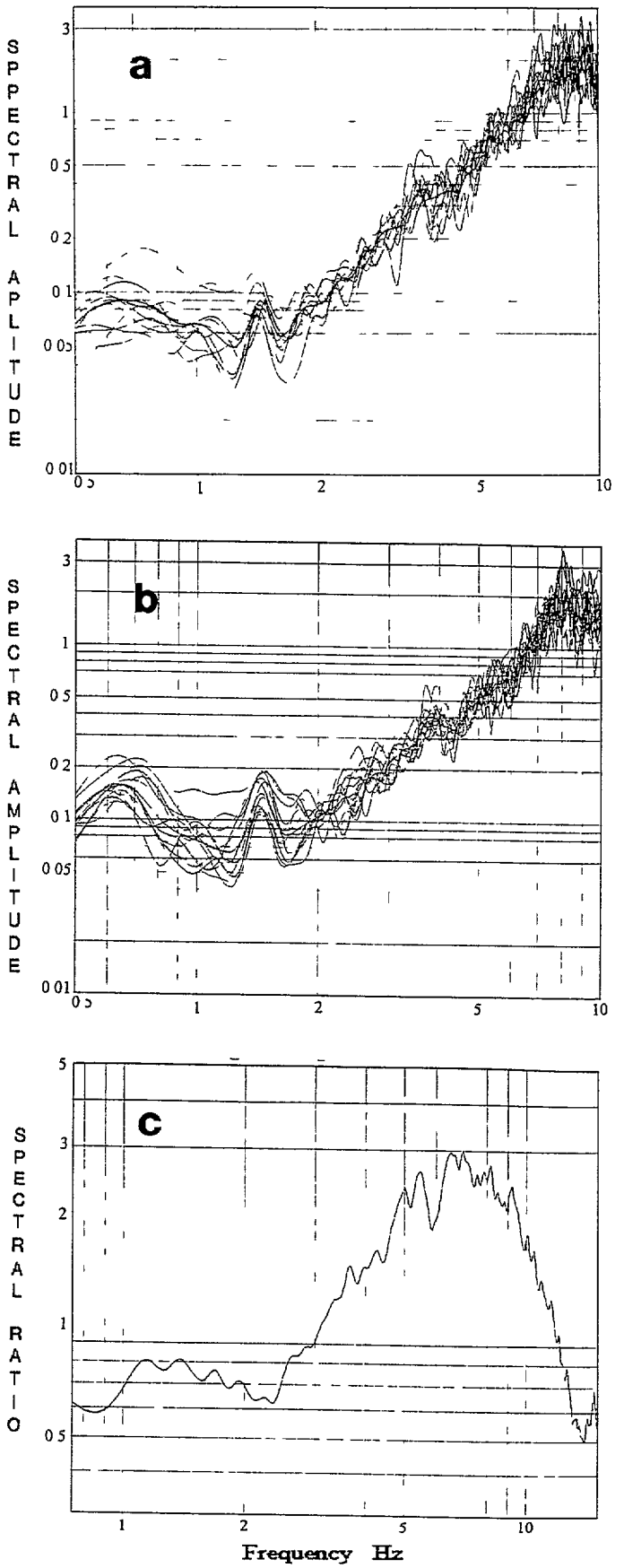


Figure C5 Time change of horizontal spectrum of microtremors recorded at Site 54 (a) for NS component, (b) for EW component and (c) average horizontal-to-vertical spectral ratios

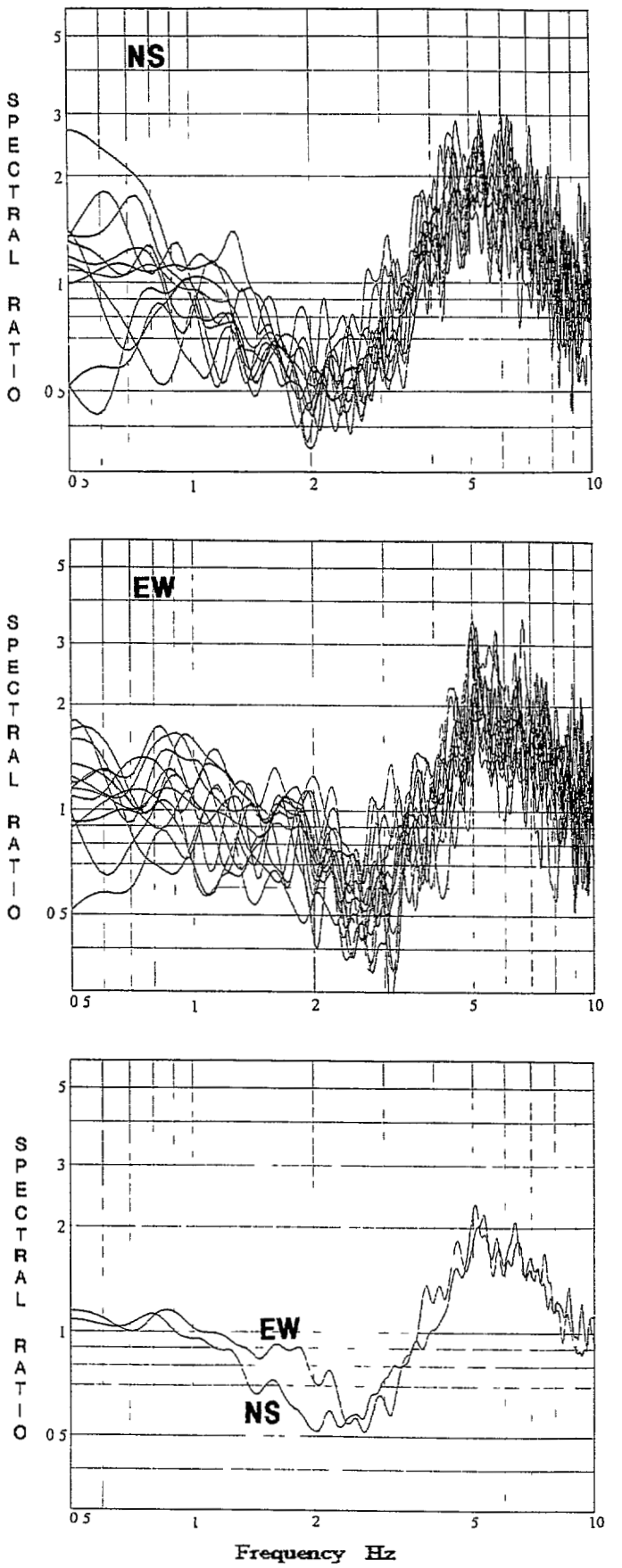


Figure C6 Individual and average spectral ratios (NS and EW components) obtained from microtremors observed at Site 34

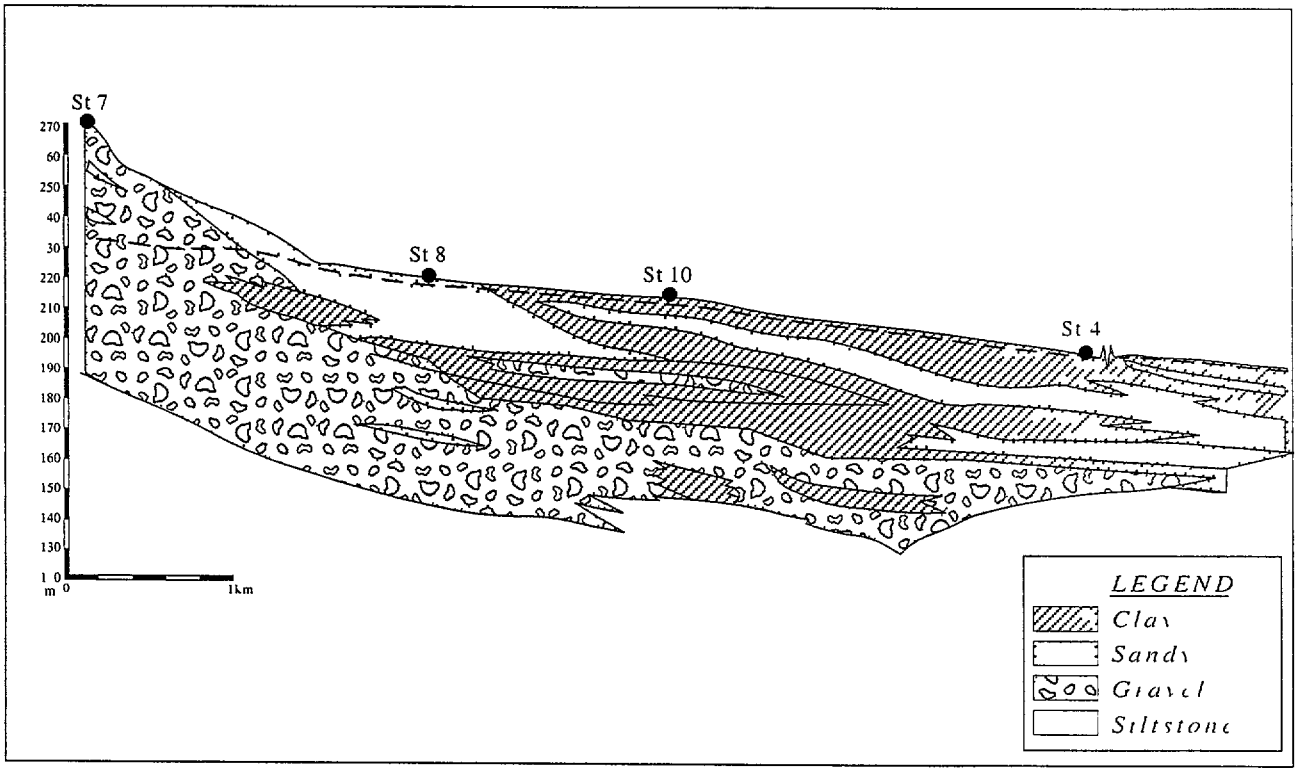


Figure C7 Example of geological cross-section for deposits of Ashgabat

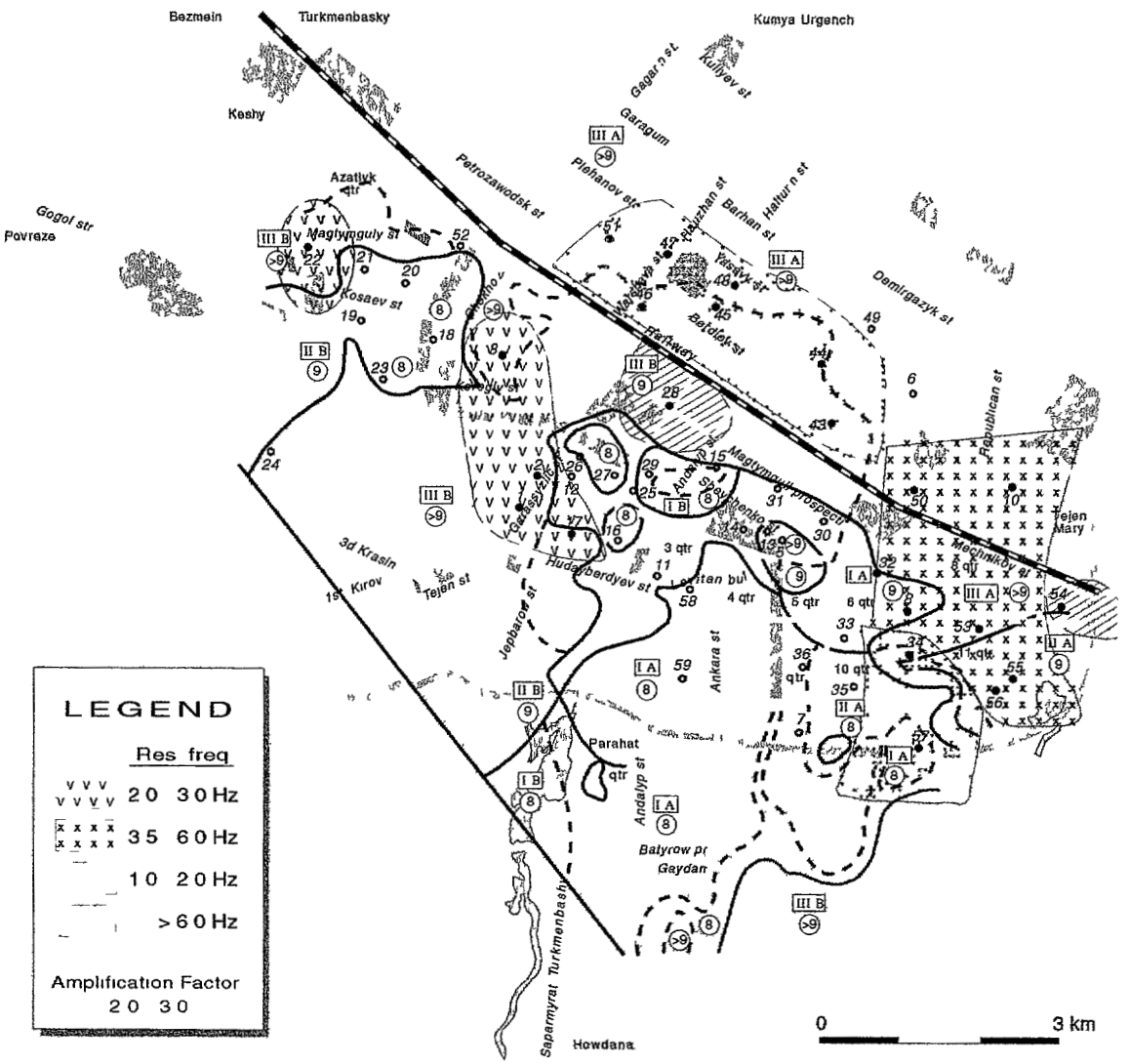


Fig 8 Distribution of fundamental frequencies estimated from H/V microtremor in Ashgabat

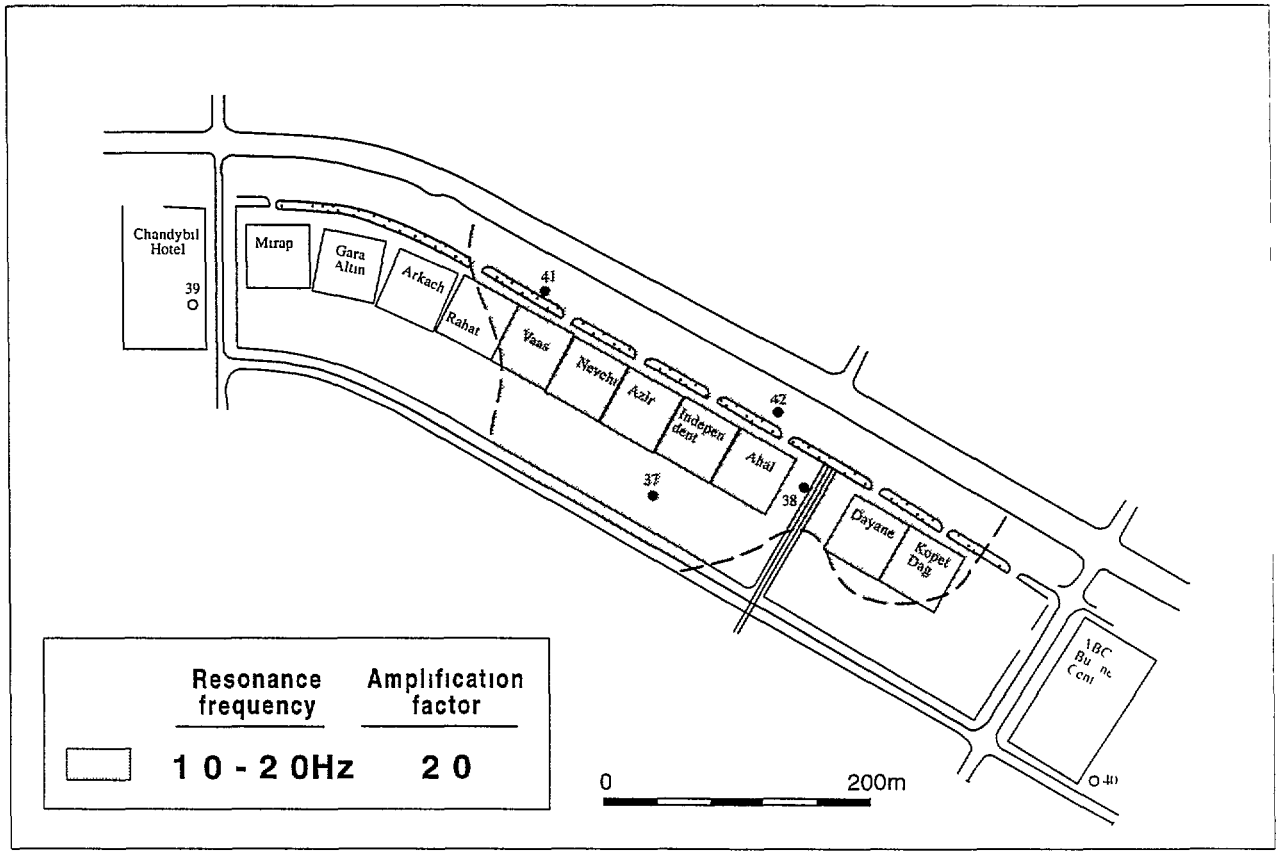


Figure C9 Distribution of fundamental frequencies estimated from H/V ratio of microtremors at Hotel area in Ashgabat

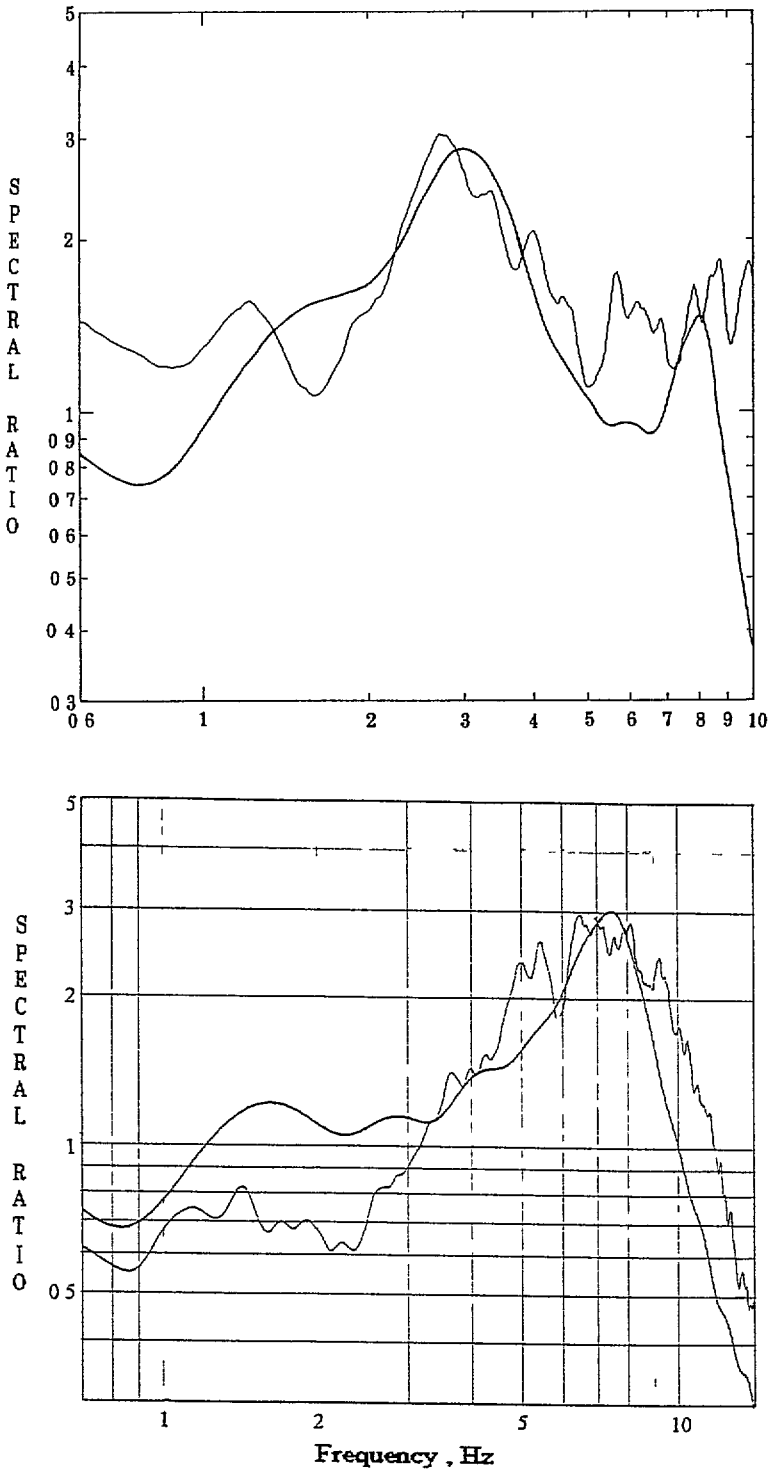


Figure C10 Comparison of site response estimates obtained at Zones 2 and 4 average empirical transfer functions (thin line) and theoretical transfer function (heavy line) computed for model with two layers over a half-space

Appendix D

# DYNAMIC CHARACTERISTICS OF RESIDENTIAL BUILDINGS IN ASHGABAT, TURKMENISTAN

## RATIONALE

Earthquake risk analysis depends heavily on our capability to assess the vulnerability of existing buildings to ground shaking It seems that the engineering community has the knowledge and computational means to perform such an analysis on an individual basis (one specific building) When considering an area or a town, however, the problem is still far from being resolved and most of the proposed solutions are based on statistical analysis of the damage (seismic intensities) caused by previous earthquakes This approach, however, may not be valid in certain cases, like that of Ashgabat, where the engineering characteristics of existing buildings are different from those that were exposed to previous earthquakes

The current study adheres to the general concept that the vulnerability of a building to ground shaking is governed primarily by the resonance effect, i e , the displacements and accelerations developed on the building at frequencies that are close to its natural frequencies of motion Consequently, an important step toward better evaluations of the earthquake risk is associated with determining the dynamic parameters of existing buildings The dynamic characteristics of real structures can be determined experimentally using very simple and inexpensive measurements by monitoring the shaking of the structure caused by ambient noise (Zaslavsky, 1989, Zaslavsky and Shapira, 1994, Zaslavsky and Shapira, 1997, Zaslavsky et al , 1997, 1998, Pardoen, 1988, Carudis and Mouzakis, 1986, Luco et al , 1987, Bongiovanni et al , 1987, Mendosa et al , 1991, Celebi et al , 1993 and others)

The first, but very modest, attempt to characterize the dynamic properties of existing buildings in Ashgabat was made in the framework of this project It concerns a study of only three buildings that seem to be prototypes of many residential buildings constructed in Ashgabat after the destructive earthquake of 1948 and especially in recent years At this stage, we concentrate our attention on the problem of estimating the natural frequency of motion of a building as a function of its height

## THE EXPERIMENT

Two modern prefabricated residential buildings and one old stone building were temporarily instrumented with three seismograph stations The stations were located on the

roof and in the basement of each building Each location was equipped with a pair of horizontal seismometers, placed perpendicular to each other and parallel to the outer walls of the structure Fig D1 is a schematic description of the instrumented buildings and the configuration of measured sites The first prefabricated building is located at 36 Andalib Street, it is four stories high (16 meters) and is rectangular in shape (12x24 meters) The second prefabricated building is located at 14 Peace Avenue This building is nine stories high (28 meters) and also rectangular (20x14 meters) The elevators and stairway are integral to the structure The stone house, located at 13 Mollanepes Street, is two stories high and its dimensions are 9x15 meters and 7 meters in height

The monitoring system is based on the PC-SDA (Shapira and Avirav, 1997) that was designed in the framework of the US-AID project Each recording session was three minutes long and automatically repeated every 15 minutes over period a period of about eight hours Spectra computations comprised a time window of 40 sec By means of trial and error, we concluded that this time window is sufficient to provide stable results The selected time windows were Fourier transformed, using cosine-tapering before transformation and then smoothed with a triangular moving Hanning window (0 4 Hz) and re-sampled every 0 048 Hz in the 0 5-20 Hz frequency band The characteristic spectrum of each measured point and for each seismometer, was obtained by averaging the spectral amplitudes of many spectra

## ANALYSIS AND RESULTS

### *FOUR STORY BUILDING*

Individual and average amplitude spectra of ambient noise measured at Stations 1 and 2 on the roof are shown in Fig D2 The highest spectral amplitudes are observed at 5 6 Hz (for the NS direction) and 4 95 Hz (for the EW direction)) These frequencies are interpreted as the fundamental translation motions of the structure in these directions (first modes) Comparison of spectra of the vibrations in the NS direction at Stations 1 and 2 shows that a frequency of 6 8 Hz should be attributed to the main torsion mode of the structure The torsion effect is indicated by the different spectral levels (same direction) between Station 1 (center of the roof) and Station 2 (near the exterior wall) At this point it should be emphasized that similar frequencies were interpreted from different groups of records obtained at different times of the day The observed standard deviations are 0 04 Hz and 0 05 Hz for the NS and the EW

directions, respectively These very low uncertainty estimates clearly demonstrate the high resolution than can be achieved by the applied method

The damping ratios (a manifestation of the stiffness of the structure) that correspond to the fundamental modes of vibration are estimated from the width of the spectral peak

$$\xi = (f_2 - f_1)/2f_0 \tag{D-1}$$

or

$$\xi = (f_2 - f_1)/(f_2 + f_1) \tag{D-2}$$

where $\xi$ is the critical damping ratio, $f_0$ is the modal frequency, $f_1$ and $f_2$ are the frequencies corresponding to the bandwidth at 75% of the spectral amplitude at the frequency $f_0$
The estimated damping ratio for both the NS and EW components are only 1 0-1 2%

*NINE STORY BUILDING*

Fig D3 shows the average amplitude spectrum of the ambient excitation in an EW direction that were monitored on the roof of the building The dominant feature of the spectra is a maximum at the frequency f=2 8 Hz This peak is associated with the fundamental translation motion in the EW direction A second peak at f =8 7 Hz corresponds to the second mode in that direction The spectral peaks at frequencies f=3 6 Hz and 10 3 Hz, which are clearly seen in the spectra of the ambient motions at Station 2, correspond to the first and second torsion modes Examples of the individual and average spectra that were obtained from measurements in the NS direction at Station 2, are shown in Fig D4 The observed dominant frequencies at f=2 8 Hz and f=9 0 Hz correspond to the first and second modes in that direction Note that the two significant modal frequencies in each of the principal axis of the building follow the general approximation of *f* and *3f*

Based on equation (D-1), the estimated damping ratios for the first modes in the NS and the EW directions are 2 5% and for first torsion mode it is 1 5%

*TWO STORY BUILDING*

Individual and average spectra of ambient motions in the NS and the EW directions are shown in Fig D5 The spectra reveal two distinct peaks at 7 6 Hz (for NS direction) and at

8 0 Hz (for EW direction) These frequencies are interpreted as the fundamental modes along both horizontal axes of the building The damping at these fundamental frequencies is 3 5%

## DISCUSSION

The use of relatively simple spectral analysis techniques of low amplitude seismic motions facilitates the determination of the fundamental dynamic characteristics of buildings The results are summarized in Table D1

**Table D1 - Natural Frequencies and Damping Ratios of Selected Buildings**

| Building | Mode | Frequency (Hz) | Damping ratio (%) |
|---|---|---|---|
| 9 story | First mode NS direction | 2 8 | 2 5 |
| | First mode EW direction | 2 8 | 2 5 |
| | First torsional | 3 6 | 1 5 |
| | Second mode NS direction | 9 0 | - |
| | Second mode EW direction | 8 7 | - |
| | Second torsional | 10 3 | - |
| 4 story | First mode NS direction | 5 6 | 3 5 |
| | First mode EW direction | 4 95 | 3 5 |
| | First torsional | 6 8 | - |
| 2 story | First mode NS direction | 7 6 | 3 5 |
| | First mode EW direction | 8 0 | 3 5 |

Assuming that the earthquake vulnerability of a building is basically a function of the ground vibrations at its natural frequency that, in turn, is a function of its height In many building codes (see for example Luft, 1980) the natural frequency of a structure is estimated, to the first order, by the formula

$$f = 10/N \qquad \text{(D-3)}$$

where N is the number of stories This formula is widely used in studies associated with seismic risk assessment and earthquake scenarios for estimating expected economic loss from earthquakes Equation (D-3) predicts natural frequencies of 1 1, 2 5 and 5 Hz for the nine, four

and two story building, respectively The differences between these estimations and the observed natural frequencies of the buildings are significant and may be critical in terms of vulnerability to seismic loads

Based on our observations, although limited, we suggest the following relationship for prefabricated buildings in Ashgabat

$$f = 23/N \tag{D-4}$$

It has been demonstrated that the recorded response of buildings to ambient excitation yields accurate determinations of the fundamental (translational and torsion) frequencies and damping Consequently, we may suggest that

1 The empirical results be used for better modeling of the behavior of buildings in Ashgabat under the exposure to seismic loads
2 Similar measurements should be conducted on other building to verify our initial approximations
3 The dynamic characteristics obtained using the spectral analysis technique should be compared with characteristics from future periodic test Repeated measurements may be used to detect changes in the dynamic properties of a structure that, in turn, are indicative of a possible increase in the vulnerability to seismic vibrations

## REFERENCES

Bongiovanni, G , Celebi, M and Safak, E , 1987 Seismic rocking response of a triangular building founded on sand, *Earthquake Spectra*, Vol 3, No 4, 793-809

Carudis, P and Mouzakis, H P , 1986 Small amplitude vibration measurements of buildings undamaged, damaged and repaired after earthquakes, *Earthquake Spectra*, Vol 2, No 3, 515-535

Celebi, M , Plan, L T and Marshall, R D , 1993 Dynamic characteristics of five tall buildings during strong and low-amplitude motion, *The Structural Design of Tall Buildings*, Vol 2 1-15

Luco, J E , Trifunac, M D and Wong, H L , 1987 On the apparent change in dynamic behavior of the nine story reinforced concrete building, *Bull Seism Soc Am* 77 1961-1983

Luft, R W , 1989 Comparison among earthquake codes, *Earthquake Spectra*, Vol 5, No 5, 767-789

Mendosa, L , Reyes, A and Luco, J E , 1991 Ambient vibration test of the Mexican general hospital, *Earthquake Spectra*, Vol 7, 281-300

Pardoen, G C , 1983 Ambient vibration test of the Imperial County Services Building, *Bull Seism Soc Am* , 73 1895-1902

Shapira, A , and Avirav, V , 1995 PC-SDA operation manual, IPRG Rep No Z1/567/79

Zaslavsky, Y , 1989 Full scale investigation of the Nurek Dam vibrations, improvement of reliability of energetic structures under the influence of dynamic, *Energoatomizdat*, 12-17

Zaslavsky, Y and Shapira, A , 1994 Empirical determination of the dynamic characteristics of a reinforced concrete construction, 17th European Seminar on Earthquake Engineering, Haifa, Proceedings, 499-508

Zaslavsky, Y and Shapira, A , 1997 Empirical estimates of modal parameters of full scale structures, *European Earthquake Engineering*, No 1, 26-36

Zaslavsky, Y , Shapira, A and Pinsky, V , 1997 Evaluation of seismo-engineering parameters for earthquake risk and loss assessment, Proceeding of 8th International Conference on Soil Dynamics and Earthquake Engineering, Istanbul, July 20-24

Zaslavsky, Y , Shapira, A and Pinsky, V , 1998 Dynamic characteristics of two three-story buildings obtained by seismological measurements, Proceeding of XXVI General Assembly of the European Seismological Commission (ESC), Tel Aviv, Israel, August 23-28, 213-217

# FIGURE CAPTIONS

Figure D1 Station configuration during various tests

Figure D2 Individual and averaged amplitude spectra of ambient noise measured at Stations 1 and 2 on the roof of the four story building

Figure D3 Average amplitude spectrum (EW direction) of ambient noise at Stations 1 and 2 on the roof of the nine story building

Figure D4 Individual and averaged amplitude spectra of ambient noise measured at Station 2 (NS direction) on the nine story building

Figure D5 Individual and averaged amplitude spectra of ambient noise, measured at the two story building

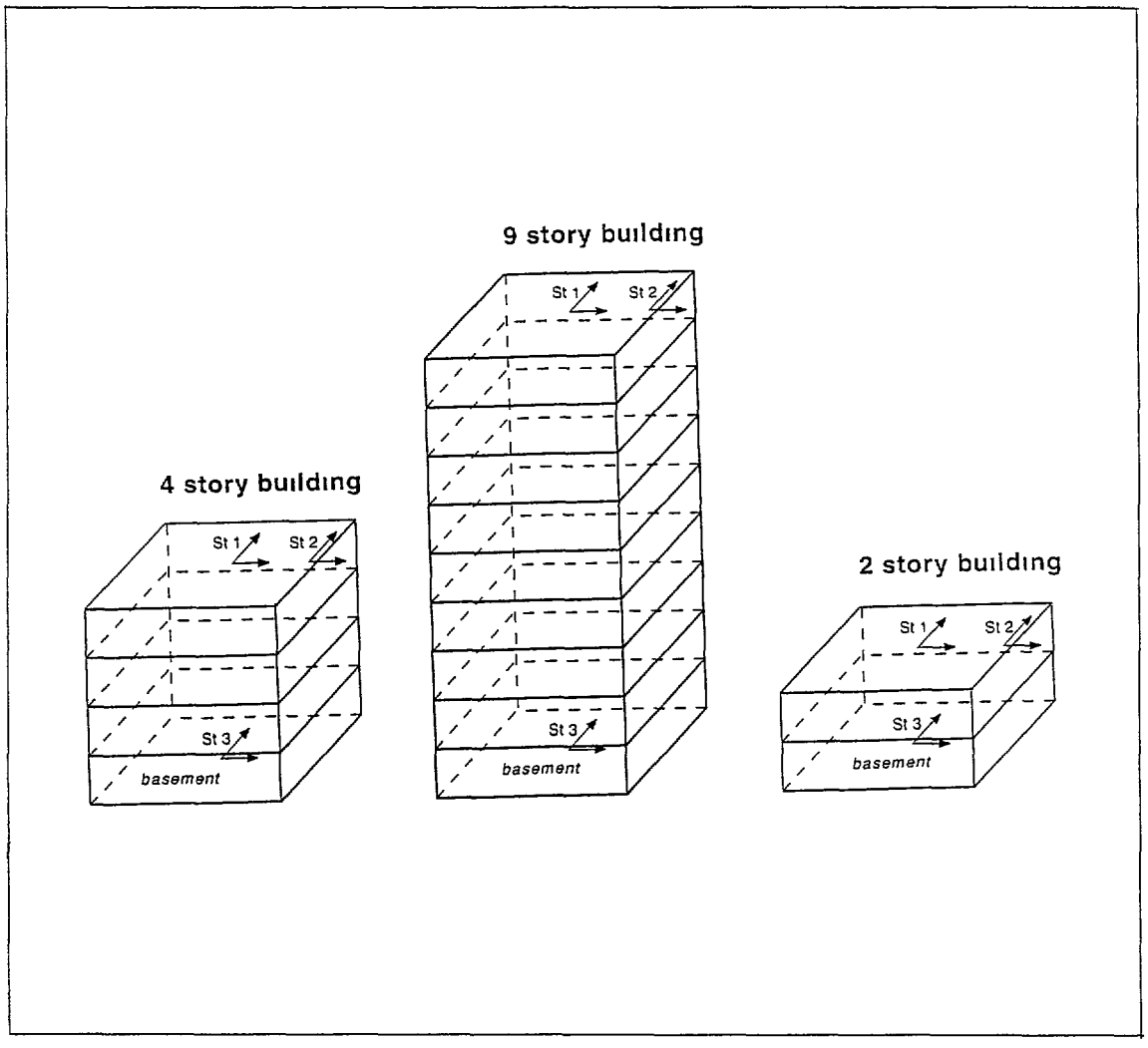


Figure D1 Station configuration during various tests

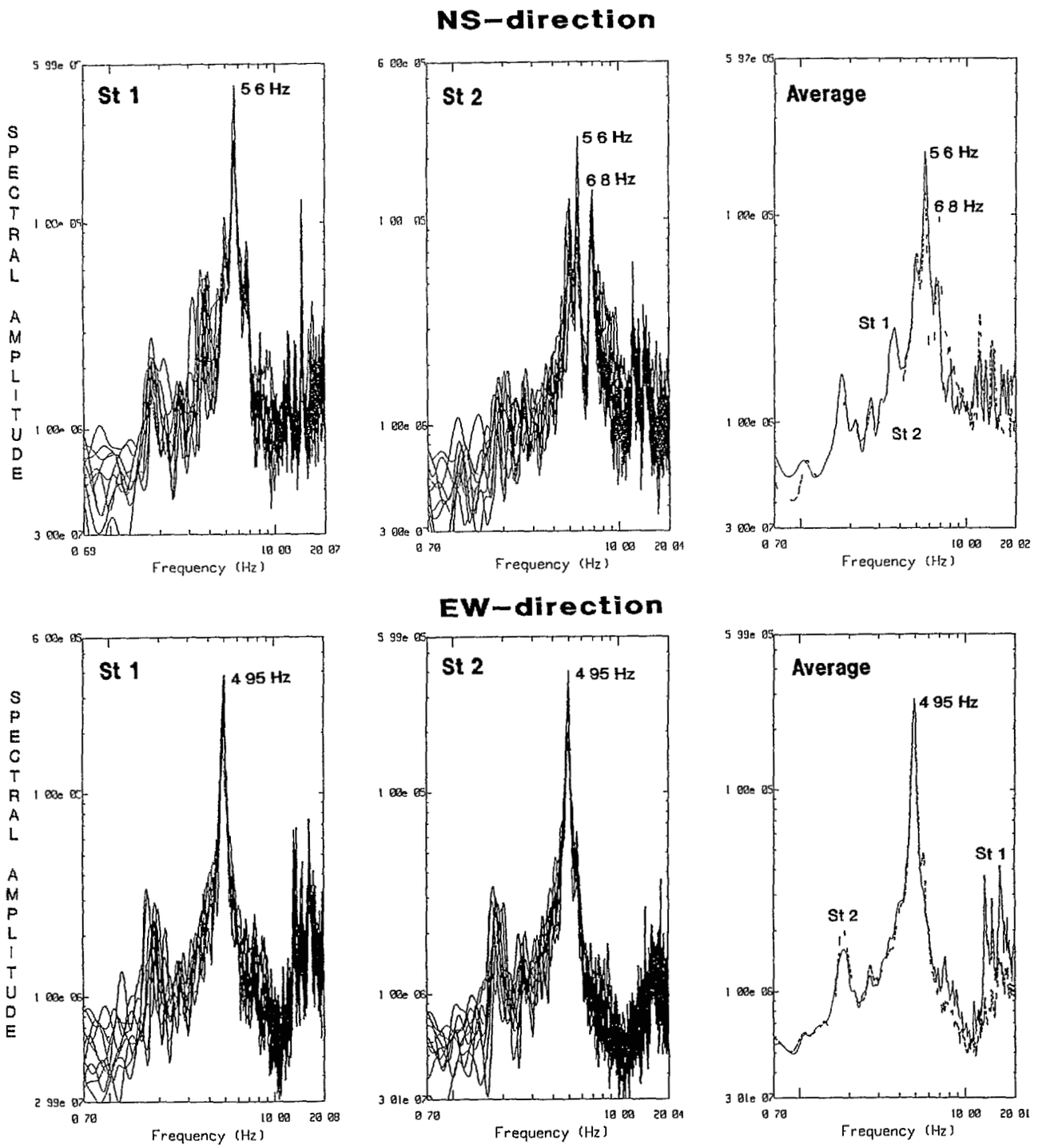


Figure D2 Individual and averaged amplitude spectra of ambient noise measured at Stations 1 and 2 on the roof of the four story building

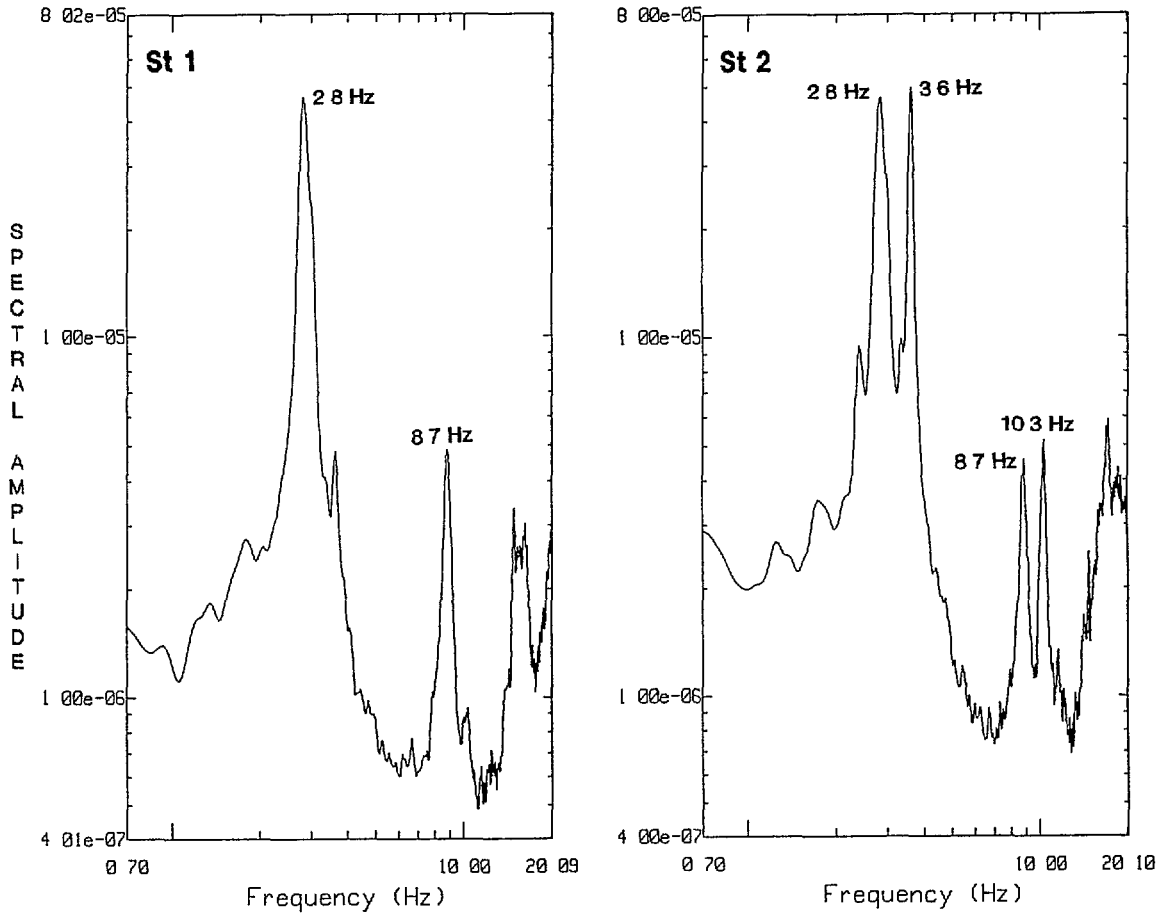


Figure D3 Average amplitude spectrum (EW direction) of ambient noise at Stations 1 and 2 on the roof of the nine story building

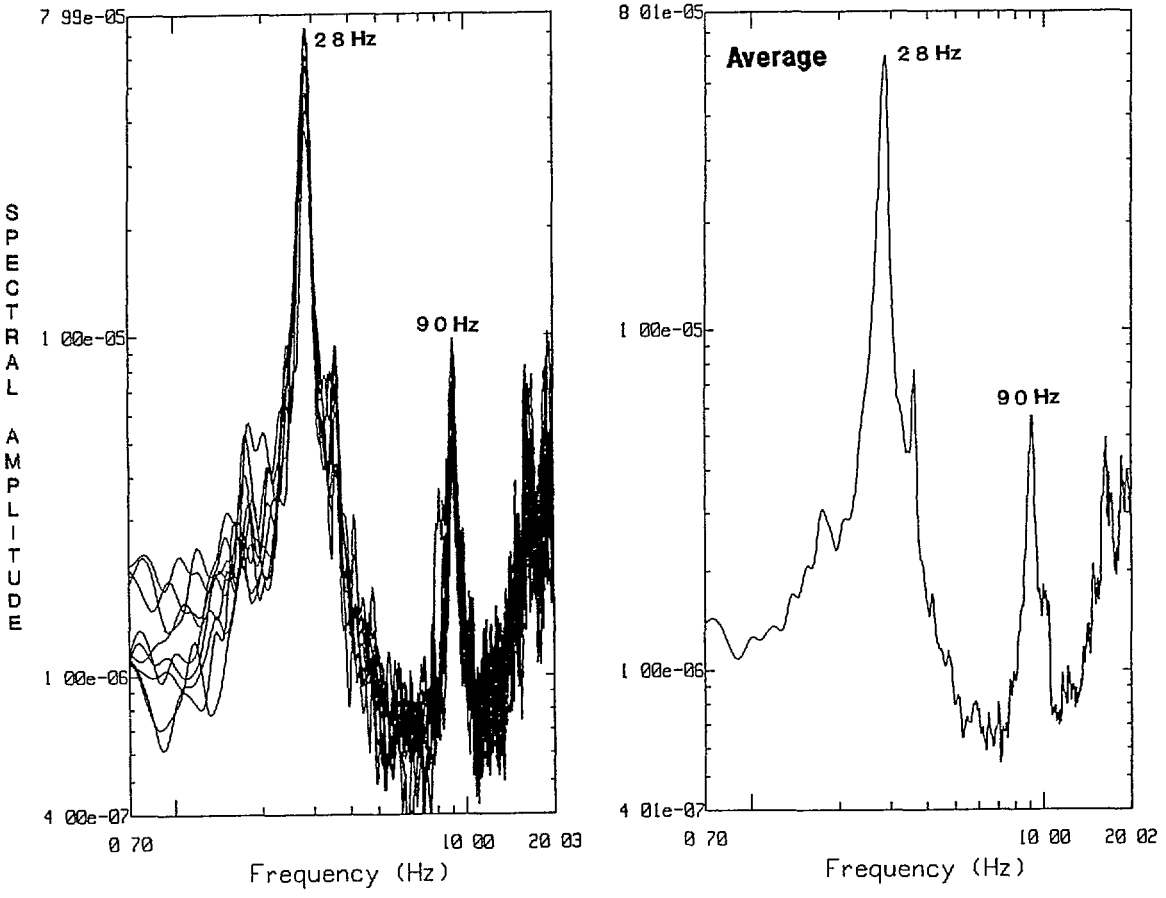


Figure D4 Individual and averaged amplitude spectra of ambient noise measured at Station 2 (NS direction) on the nine story building

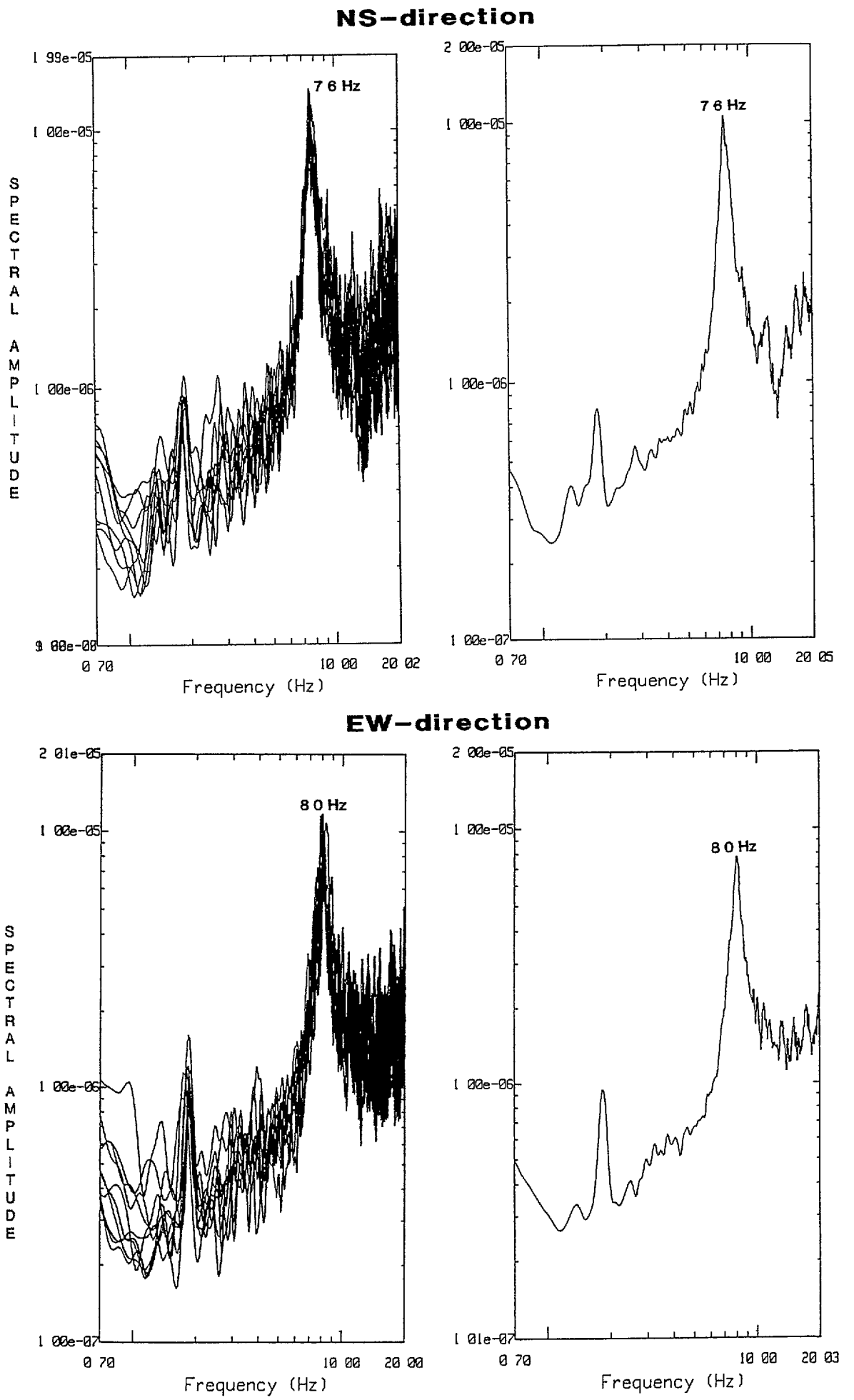


Figure D5 Individual and averaged amplitude spectra of ambient noise, measured at the two story building